# Soil Development and Nutrient Availability Along a 2 Million-Year Coastal Dune Chronosequence Under Species-Rich Mediterranean Shrubland in Southwestern Australia

## Benjamin L. Turner & Etienne Laliberté

ECOSYSTEMS

Storm Events and Whole-lake
CO$_2$ Dynamics

Elephant Impacts on
Functional Diversity of Trees

Representing Habitat
Heterogeneity in Spatial Food
Web Models

Herbivores Sharpen
Boundaries Between Terrestrial
and Aquatic Ecosystems

Biogeochemical Hotspots in
Forested Landscapes

Springer

Springer

**ECOSYSTEMS**

# Soil Development and Nutrient Availability Along a 2 Million-Year Coastal Dune Chronosequence Under Species-Rich Mediterranean Shrubland in Southwestern Australia

Benjamin L. Turner[1]* and Etienne Laliberté[2]

[1]Smithsonian Tropical Research Institute, Apartado 0843-03092, Balboa, Ancon, Republic of Panama; [2]School of Plant Biology, The University of Western Australia, Crawley, Perth, Western Australia 6009, Australia

## ABSTRACT

Soil chronosequences provide valuable model systems to investigate pedogenesis and associated effects of nutrient availability on biological communities. However, long-term chronosequences occurring under seasonally dry climates remain scarce. We assessed soil development and nutrient dynamics along the Jurien Bay chronosequence, a 2 million-year sequence of coastal dunes in southwestern Australia. The chronosequence is significant because it occurs in a Mediterranean climate and supports hyperdiverse shrublands within a global biodiversity hotspot. Young soils formed during the Holocene ($<6,500$ years old) are strongly alkaline and contain abundant carbonate, which is leached from the profile within a few thousand years. Middle Pleistocene soils (ca 120,000–500,000 years old) are yellow decalcified sands with residual iron oxide coatings on quartz grains over a petrocalcic horizon that occurs at increasing depth as soils age. Early Pleistocene soils ($>2,000,000$ years old) are completely leached of iron oxides and consist of bleached quartz sand several meters deep. Changes in soil organic matter and nutrient status along the Jurien Bay chronosequence are consistent with patterns observed along other long-term chronosequences and correspond closely to expectations of the Walker and Syers (1976) model of biogeochemical change during pedogenesis. Organic carbon and nitrogen (N) accumulate rapidly to maximum amounts in intermediate-aged Holocene dunes and then decline as soils age. In contrast, total phosphorus (P) declines continuously along the chronosequence to extremely low levels after 2 million years of pedogenesis, eventually representing some of the lowest P soils globally. Ratios of soil organic carbon to P and N to P increase continuously along the chronosequence, consistent with a shift from N limitation on young soils to extreme P limitation on old soils. Phosphorus fractionation by sequential extraction reveals a rapid decline in primary and non-occluded phosphate and an increase in organic and occluded P as soils age. Concentrations of extractable (that is,

readily bioavailable) N and P, as well as exchangeable cations, are greatest in Holocene dunes and decline to low levels in Pleistocene dunes. Extractable micronutrient concentrations were generally very low and varied little across the chronosequence. We conclude that the Jurien Bay chronosequence is an important example of changing patterns of nutrient limitation linked to long-term soil and ecosystem development under a Mediterranean climate.

## INTRODUCTION

A soil chronosequence is a series of soils that differ from each other only in the time since the onset of their formation (Stevens and Walker 1970; Vitousek 2004). Other soil-forming factors, including parent material, topography, climate, and vegetation, are held relatively constant, although it is recognized that climate and vegetation rarely conform strictly to this definition (Huggett 1998). Nevertheless, soil chronosequences provide an important means of assessing pedogenesis and associated patterns of nutrient availability and limitation in terrestrial ecosystems over timescales from hundreds to millions of years (Vitousek 2004; Walker and others 2010; Turner and Condron 2013).

Typically, nutrient availability follows a predictable pattern during long-term pedogenesis (Walker and Syers 1976). Nitrogen (N) is absent from most parent materials, but accumulates quickly in young soils through biological N fixation (Menge and Hedin 2009). In contrast, phosphorus (P) declines continually as pedogenesis proceeds, as it is lost in runoff at a greater rate than it is supplied by bedrock weathering and atmospheric deposition (Walker and Syers 1976). At the same time, chemical and biological transformations further reduce the availability of the P remaining in the soil by converting primary mineral phosphate into organic forms and occluding them within secondary minerals (Walker and Syers 1976; Parfitt and others 2005; Turner and others 2007). As a result, primary productivity tends to be limited by N availability on young soils and by P availability on old soils (Vitousek and Farrington 1997; Laliberté and others 2012; Coomes and others 2013). In very old soils on stable landscapes, P limitation can become strong enough to constrain plant biomass, productivity, and other ecosystem processes, termed 'ecosystem retrogression' (Wardle and others 2004), and to influence the distribution and diversity of plant and microbial communities (Williamson and others 2005; Lambers and others 2008; Jangid and others 2013; Laliberté and others 2013a, 2014).

Long-term retrogressive soil chronosequences have been identified in only a few locations around the world (Peltzer and others 2010). Well-known examples are the Hawaiian Islands chronosequence (Crews and others 1995; Vitousek 2004), the Franz Josef post-glacial chronosequence in New Zealand (Walker and Syers 1976), and the Cooloola coastal dune chronosequence in eastern Australia (Thompson 1981). However, the majority of these chronosequences occur in relatively humid climates, with only a small number in more arid ecosystems. These include the 3 million-year San Joaquin alluvial terrace sequence under Mediterranean grassland in California (Harden 1982; Baisden and others 2002) and the 3 million-year basalt chronosequence in the Northern Arizona Volcanic Field, which supports a semiarid piñon–juniper woodland (Selmants and Hart 2008, 2010).

Long-term nutrient dynamics might be expected to deviate from the Walker and Syers (1976) model in dry ecosystems through a slower rate of P loss by leaching (Lajtha and Schlesinger 1988). However, both the Northern Arizona and the San Joaquin chronosequences show patterns of soil nutrients that are consistent with the Walker and Syers model of nutrient dynamics during pedogenesis. Additional information from similar arid environments around the world, which includes much of the Australian continent, is required to confirm the broad applicability of the Walker and Syers (1976) model to Mediterranean ecosystems.

Here we report the results of a study of soils along a 2 million-year coastal dune chronosequence at Jurien Bay, Western Australia. The chronosequence occurs under a Mediterranean climate but differs from the previously studied dry chronosequences in terms of its origin and parent material (coastal carbonate dunes) and is of particular interest because of the exceptionally high levels of plant diversity due to its location within a global biodiversity hotspot (the Southwest

Australian Floristic Region) (Hopper and Gioia 2004). A glasshouse nutrient-addition experiment using soils from the Jurien Bay chronosequence found evidence for a shift from N to P limitation (Laliberté and others 2012), which was supported by a subsequent analysis of foliar nutrient concentrations and resorption efficiency in naturally occurring plants in the field (Hayes and others 2014). Here we report the results of a detailed assessment of (i) pedogenesis through soil profile descriptions and nutrient budgets, (ii) the dynamics of organic matter, (iii) amounts and composition of soil P, and (iv) biologically available nutrient concentrations, including N, P, major cations, and micronutrients.

## THE JURIEN BAY CHRONOSEQUENCE

The 2 million-year Jurien Bay dune chronosequence is located in southwestern Australia, approximately 200 km north of Perth (30°01′–30°24′ south, 114°57′–115°11′ east; Figure 1A). The chronosequence is part of the Swan Coastal Plain, where a series of coastal sand deposits run parallel to the coastline for approximately 400 km from Busselton in the south to Jurien Bay in the north (McArthur and Bettenay 1974; McArthur 2004). The sand deposits were formed by sea level fluctuations since the Early Pleistocene (or possibly Late Pliocene), approximately 2.59 million years ago (Kendrick and others 1991; Laliberté and others 2012). The Swan Coastal Plain lies within the Perth Basin, which extends approximately 1000 km north–south along the coast of southwestern Australia. The Perth Basin is bounded to

the east by the Darling Fault, which separates it from the Archean Yilgarn Block, part of the Western Australian Shield (Playford and others 1976).

Coastal dune soils in the Swan Coastal Plain have been grouped into three main units based on the corresponding dune systems (McArthur and Bettenay 1974; McArthur 2004; Laliberté and others 2012). The three dune systems (Quindalup, Spearwood, and Bassendean) correspond generally with the Safety Bay Sand, the Tamala Limestone, and the Bassendean Sand, respectively (Table 1) (Playford and others 1976).We delineated six main chronosequence stages within these three dune systems (see below). The Spearwood and Bassendean dunes are more than 20 km wide in places along the Swan Coastal Plain, although the Bassendean dunes disappear abruptly north of the Jurien Bay area. Below we describe the Jurien Bay chronosequence in the context of the major soil-forming factors of time, parent material, climate, vegetation, and topography (Jenny 1941), as well as the influence of disturbance on the integrity of the chronosequence.

### Ages of Dune Formation

Sea level changes during the Quaternary are now well established based on marine oxygen isotope records (for example, Lambeck and Chappell 2001; Berger 2008; Lewis and others 2013) and provide the basis for understanding coastal dune succession along the Jurien Bay chronosequence. Sea level has lowered progressively since the Miocene, punctuated by periodic sea level high stands associated with interglacial periods (Miller and others
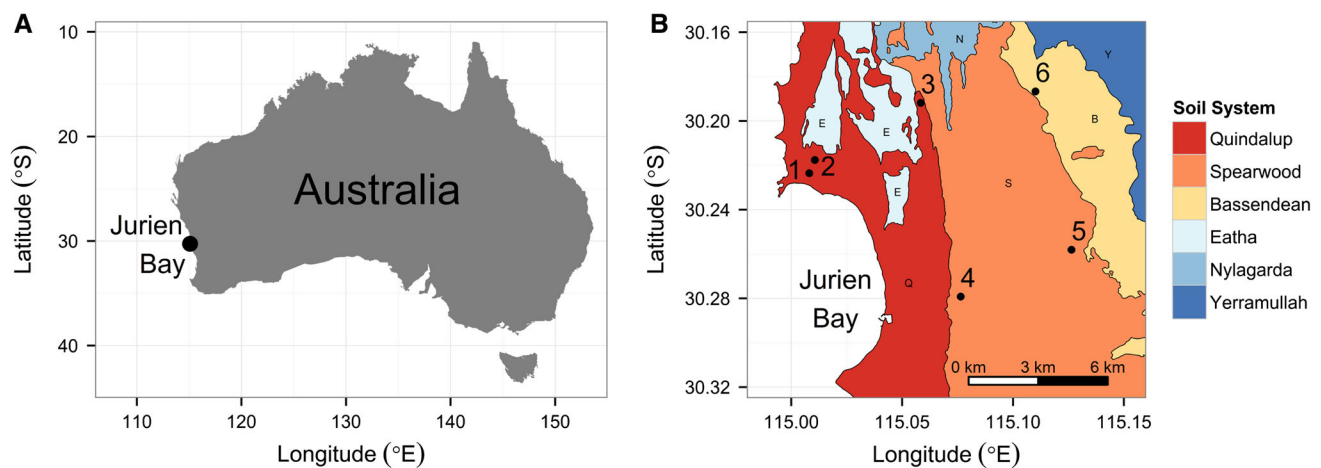


**Figure 1.** Map of Australia (**A**), showing the location of the Jurien Bay chronosequence, and a detailed map of the Jurien Bay area (**B**), showing the three main dune systems (Quindalup, Spearwood, and Bassendean) and the locations of the six profile pits. Note that the Eatha, Nylagarda, and Yerramullah soils are not part of the chronosequence.

B. L. Turner and E. Laliberté

**Table 1.** The Three Main Phases of Dune Development Along the Jurien Bay Chronosequence, South-western Australia

| Dune system | Dune ages | Chronosequence stages | Years before present | Marine isotope stage | Associated geological formation | Nature of soils |
|---|---|---|---|---|---|---|
| Quindalup | Holocene | 1, 2, 3 | <6,500 | 1 | Safety Bay Sand | Calcareous sand |
| Spearwood | Middle Pleistocene | 4, 5 | 120,000–500,000 | 5e to 13 | Tamala Limestone | Decalcified sand with residual iron oxides over indurated limestone |
| Bassendean | Early Pleistocene (and possibly Late Pliocene) | 6 | >2,000,000 | – | Ascot Formation | Residual quartz sand; parent material probably contained less carbonate than Quindalup or Spearwood |

2005). The major dune units that occur along the Jurien Bay chronosequence most likely correspond with the greatest sea level high stands, with dunes formed during lower-level high-stands being reworked or submerged by subsequent high stands (Brooke and others 2014).

Coastal dunes in southwestern Australia represent three main phases of dune development associated with global sea level high stands during the Holocene, Middle Pleistocene, and Early Pleistocene (Table 1). Even older sand deposits, the Yoganup Formation, occur in the region at the foot of the Darling Escarpment (Kendrick and others 1991). The formation is probably older than Pliocene but is not well understood and is not included in the Jurien Bay chronosequence, which extends only to deposits ranging in age from the present to the Early Pleistocene, or possibly Late Pliocene (Kendrick and others 1991).

The oldest deposits along the Jurien Bay chronosequence are the Bassendean dunes. These have been assigned an Early Pleistocene age based on their interpretation as the dune facies of the underlying Ascot Formation, which has been dated by marine fossil assemblages (Kendrick and others 1991).

The Spearwood dunes formed during the Middle Pleistocene, ca 120,000–500,000 years ago. Based on heavy mineral assemblages, five Spearwood dune sub-systems have been recognized in the Perth area (with increasing age from west to east, the Trigg, Karrinyup, Gwelup, Balcatta, and Yokine Dunes) (Bastian 1996), although they have proven difficult to date precisely (Hewgill and others 1983; Murray-Wallace and Kimber 1989; Price and others 2001; Hearty and O'Leary 2008). However, there is widespread agreement that the youngest Spearwood dune system corresponds to the last interglacial sea level high stand (Marine Isotope Stage (MIS) 5e, ca 116,000–128,000 years ago) (Stirling

and others 1998), and the increasing age of the dune systems with progression inland is supported by several lines of evidence, including heavy mineral assemblages and dating by thermoluminescence, optically stimulated luminescence, electron-spin resonance, and amino-acid racemization (Bastian 1996; Price and others 2001; Hearty and O'Leary 2008; Brooke and others 2014). Older dunes presumably correspond to earlier major sea level high stands, which occurred at approximately 220,000 years (MIS 7), 330,000 years (MIS 9), 410,000 years (MIS 11), and 480,000 years (MIS 13) (Lisiecki and Raymo 2005). The upper age of the Spearwood dunes is constrained at about 500,000 years by optical luminescence dating (Brooke and others 2014). As sea level high stands prior to about 500,000 years were relatively low, it is presumed that older deposits (but younger than the Bassendean dunes) were below the current sea level and subsequently destroyed by Middle Pleistocene high stands (Hearty and O'Leary 2008).

The Quindalup dunes (McArthur and Bettenay 1974) are the most recent dune system, formed in the last 6,500 years since the Holocene post-glacial sea level high stand (Woods and Searle 1983). Although at least four phases of Quindalup dune development have been identified in areas of the Swan Coastal Plain (McArthur 2004), we grouped the Holocene dunes at Jurien Bay into three age classes based on the degree of soil development and landscape position (Hayes and others 2014). Young Quindalup dunes are no more than 100 years old, have been only recently stabilized by vegetation, and exhibit little or no pedogenic development. Medium-aged Quindalup dunes are approximately 1,000 years old, have continuous vegetation cover, and exhibit weak but recognizable development of an epipedon in the soil profile. Old Quindalup

dunes are approximately 6,500 years old and occur inland at the Holocene–Pleistocene transition. The oldest dunes correspond to the final stages of the post-glacial marine transgression (Lewis and others 2013).

## Parent Material

The Holocene Quindalup dunes consist primarily of carbonaceous material from the nearshore coastal environment. The continental shelf off the coast of the Swan Coastal Plain is extensive and shallow, which promotes carbonate production and movement onshore during marine transgressions (Brooke and others 2014). The Spearwood dunes are thought to have formed from weathering of the underlying Tamala Limestone, a medium-to-coarse grained aeolian calcarenite (calcareous sandstone) composed of sand-sized shell fragments and quartz grains, with minor amounts of feldspars and heavy minerals including ilmenite, garnet, amphibole, and epidote, a similar composition to minerals in the Quindalup dunes (Bastian 1996). The feldspars weather rapidly and disappear, as do garnet, amphibole, and epidote, whereas ilmenite weathers to leucoxene but does not disappear (Bastian 1996). Eventually, all unstable minerals disappear, leaving almost pure quartz sand. Carbonate content in the Tamala Limestone varies from 30 to 96% (Bastian 1996; Hearty and O'Leary 2008; Brooke and others 2014).

It has been suggested that Bassendean sands might have originated as calcarenites in the same way as the Spearwood and Quindalup dunes (McArthur and Bettenay 1974; Playford and others 1976; Bastian 1996). However, it seems more likely that the Bassendean Sand contained a lower carbonate content initially, based on its association with the underlying Ascot formation (Kendrick and others 1991). This might have been due either to low carbonate production in the coastal environment at the time of deposition, or dilution by siliceous sediments from the continental landmass (Kendrick and others 1991). The extremely weathered nature of the Bassendean Sand means that it has been difficult to quantify its origin with certainty, although reference soils from the three dune systems contain similar particle size distributions, suggesting a common aeolian origin (McArthur 2004). We do not consider the possibility of a lower initial carbonate content in the Bassendean Sand to compromise studies of plant–soil interactions along the chronosequence (Laliberté and others 2013b; Hayes and others 2014), because carbonate is lost rapidly during the early stages of pedogenesis in carbonate-rich soils (for example, Salisbury 1925; Burges and Drover 1953; see below) and the younger Spearwood dunes can contain many meters of completely decalcified sand over limestone. We therefore assume that any carbonate initially present in the older Bassendean dunes would have long disappeared from the soil profile to great depth, so that the Bassendean dunes represent the endpoint of an exceptionally strong natural soil nutrient gradient for studies where slight differences in parent material can be neglected (Laliberté and others 2013b).

There have been persistent claims that the Spearwood sands originate from inland dunes that expanded onto the coastal plain during periods of aridity (that is, the desert extension hypothesis; Glassford and Killigrew 1976; Hearty and O'Leary 2008). However, this hypothesis has been refuted on the basis of a number of lines of evidence (reviewed in Laliberté and others 2013b), including the complete absence of 'desert sand' in the vast intervening areas between the purported desert source and the Swan Coastal Plain destination (Lowry 1977; Bastian 1996), a clear west-to-east trend of increased weathering of the Spearwood sands (Bastian 1996) that matches a west-to-east increase in the age of the underlying limestone (Price and others 2001; Hearty and O'Leary 2008; Brooke and others 2014), and the match in particle size distribution and mineralogy between the Spearwood dune sand and sand embedded in the underlying limestone (Wyrwoll and King 1984; Tapsell and others 2003). These separate lines of evidence confirm that the Spearwood sand is residual and originates from in situ weathering and decalcification of the Tamala Limestone, with some local remobilization but no long-range transport.

## Climate

The climate of the study area is Mediterranean, with hot, dry summers and cool, moist winters. Mean annual rainfall (measured between 1953 and 2012) is 573 mm, of which about 80% falls between May and September (Australian Bureau of Meteorology, http://www.bom.gov.au/climate/data/). There is little if any variation in rainfall along the chronosequence, which extends only an approximate 15 km inland from the coastline. The mean annual temperature is 19°C and the mean annual maximum temperature is 25°C, with February being the warmest month (mean monthly maximum of 31°C) and July the coolest (mean monthly maximum of 20°C) (data from 1969 to 2013).

In the USDA Soil Taxonomy system (Soil Survey Staff 1999), the soil-moisture regime at Jurien Bay qualifies as Xeric (that is, the soil is dry for ≥45 consecutive days in summer and moist for at least 45 consecutive days in winter), and the soil-temperature regime qualifies as Thermic (that is, the mean annual soil temperature is 15–22°C, and the difference between means of summer and winter temperatures at 50 cm below the soil surface is ≥6°C).

There is evidence that rainfall varied markedly in inland areas of Western Australia during glacial maxima, and included periods of increased aridity (for example, Fujioka and others 2009). However, the currently available evidence, although limited, suggests that climate along the coastal margins of southwestern Australia has been well buffered from conditions inland, with relatively little variation from the modern climate over the time span covered by the Jurien Bay dune chronosequence (Wyrwoll and others 2014).

## Vegetation

Vegetation in the Jurien Bay region is Mediterranean low shrubland known as kwongan (Beard 1984; Hopper 2014). The chronosequence is in the Southwest Australian Floristic Region (Hopper and Gioia 2004), which is listed as a global biodiversity hotspot (Myers and others 2000). Plant communities are dominated by schlerophyllous shrubs and trees with remarkably high species richness and endemism (Lamont and others 1984; Hopper and Gioia 2004). There is a marked increase in plant species diversity with soil age along the chronosequence (Laliberté and others 2013a, 2014). Families such as Fabaceae and Myrtaceae are common on younger dune systems, while Proteaceae become more common on older dunes (Laliberté and others 2012; Hayes and others 2014).

In agreement with evidence for a relatively stable climate along the coastal margins of southwestern Australia, there is evidence that shrublands have persisted in the region throughout the Last Glacial Maximum, whereas changes in vegetation and climate were more pronounced in the other regions of Australia that now share a similar Mediterranean climate (Dodson 2001; Barrows and Juggins 2005). Some authors have suggested that the relative climate stability in southwestern Australia (at least near the coastline) may explain why this region has retained a hyperdiverse sclerophyll flora (Hopper and Gioia 2004), whereas sclerophyll diversity was greatly reduced in southeastern Australia due to climate fluctuations during the Pleistocene (Sniderman and others 2013).

## Dune Morphology

Dune morphology varies along the chronosequence in terms of dune height and form, reflecting differences in age of the three main dune systems. The Quindalup dunes occur as marked ridges and crests with short steep slopes. In particular, the oldest Quindalup dunes form a prominent ridge that marks the transition to the much older Spearwood dunes (Laliberté and others 2012). The Spearwood dunes have clear topographic succession (see above; Bastian 1996), but dune morphology becomes subdued with distance inland. The youngest Spearwood dunes marking the Holocene–Pleistocene transition are the most prominent, with broad flattened but distinct dune ridges further inland. The Bassendean dunes retain some of their dune expression around Perth (Bastian 1996), but have generally lost their characteristic dune morphology, forming extensive flatter areas between the younger Spearwood dunes and the older laterite gravel slopes (the Peron Slopes) to the east. However, the apparently buffered climatic conditions over the Quaternary (Wyrwoll and others 2014) and the absence of 'rejuvenated' profiles in Bassendean sand (see below) suggest that the older dunes have not experienced recent extensive erosion or reworking other than at the local scale.

## Disturbance

Southwestern Australia has not been glaciated since the Permian (that is, at least 250 million years ago) (Geological Survey of Western Australia 1990). The Australian continent separated from India in the Cretaceous and from Antarctica in the Eocene, and has been drifting northward ever since (Playford and others 1976). The region is very stable geologically (Wyrwoll and others 2014), although some authors have argued that local tectonism along the coast of southwestern Australia may have influenced dune stratigraphy (Semeniuk and Searle 1986; Playford and others 2013). In general, however, the dunes have remained relatively undisturbed in their depositional settings other than local surface reworking. Importantly, they have not been buried by younger sediments and have therefore been exposed to weathering since their deposition.

Fire is the main disturbance to vegetation in the area, with typical fire-return intervals of < 30 years (Griffin and Burbidge 1990). For example, a study on the Eneabba Sandplain, around 40 km from the Jurien Bay chronosequence, estimated a mean fire-

return interval of 13 years in the last 30 years (Enright and others 2005). In these fire-prone shrublands, seedling recruitment occurs almost exclusively after fire from seeds that are either stored in the canopy (that is, serotiny; Lamont and others 1991) or as a persistent soil seed bank (Bell and others 1993). In addition, many plant species in these shrublands can re-sprout vigorously after a fire (Bell and others 1984).

We do not know of any evidence for a substantial dust imprint on the sequence (Laliberté and others 2013b), which is perhaps unsurprising given the prevailing westerly air flow from the Indian Ocean. We cannot discount greater dust inputs during glacial periods when low sea levels exposed the continental shelf. However, the extremely low total P concentrations on the oldest (Bassendean) soils, including in surface soil layers (see below), suggest the absence of long-term dust inputs. Marine aerosol inputs are presumably greater at the coast and decrease inland, although this is not reflected in exchangeable sodium concentrations, which are generally very low and are not the greatest in the youngest Quindalup soils closest to the coastline (see below).

## METHODS

### Soil Profile Pits and Plot Selection

Profile pits were excavated in August 2012 at a number of sites along the chronosequence and six of these, most clearly representing the main chronosequence stages, are described in detail here (Figure 1B; Table 1; see description of chronosequence stages below). Profiles were excavated to at least 1 m deep and up to 2 m deep for older, more developed soils. Pits were located on the shoulders or upper slopes of dunes, except for the Bassendean profile where dune morphology was indistinct. Profiles were described and sampled by genetic horizon. Profile descriptions and analytical data are presented in full in Supplementary Online Material.

To quantify changes in soil nutrients relevant to potential limitation of biological activity, we also sampled surface soils (0–20 cm depth) from 60 10 m × 10 m plots across the chronosequence (ten plots per chronosequence stage) that were selected using a random-stratified sampling design (Laliberté and others 2014). Details on plot selection and delineation of the chronosequence stages are provided elsewhere (Laliberté and others 2012, 2014; Hayes and others 2014) and are summarized here. Aerial photographs, maps (including soil, geology, and topography), and on-ground verification (for example, using soil morphological characteristics) were used to define six broad regions (chronosequence stages) corresponding to distinct dune systems of increasing age, as indicated by the degree of soil development (McArthur 2004). Stages 1–3 can be easily distinguished from stages 4–6 because the latter occur east of a distinct beach ridge that marks the transition between the Holocene and Pleistocene dunes. In addition, soils of stages 1–3 are still alkaline due to the presence of carbonates, whereas soils from stages 4–6 are decalcified (see below). Within the Holocene dunes (stages 1–3), mobile dunes (stage 1) were easily identified by their recent origin and absence of soil development. Dunes corresponding to stage 2 were located between dunes of stage 1 and 3, but are heavily vegetated, and their soils are much more developed (with an organically enriched A horizon) than those of stage 1. Older Holocene dunes (stage 3) were selected on the basis of landscape position (that is, just west of the Holocene–Pleistocene transition). Soils from stages 4–5 (Spearwood dunes) are easily distinguished by their distinct yellow color that is due to the oxidation of iron minerals. Stages 4 and 5 consist of Middle to Late Pleistocene dunes with a calcarenite core (Tamala Limestone); they show calcretes and karst-weathering profiles in the upper parts that are overlain by decalcified sand, the thickness of which depends on soil age and the degree of weathering (Bastian 1996). In stage 4, calcrete is found within 1 m of the soil surface, whereas in stage 5, it occurs at a depth of several meters or is absent in some cases (see below). Finally, dunes corresponding to stage 6 (Bassendean dunes) can be distinguished from stages 4–5 by their lack of morphological expression, gray (not yellow) sands, thick (>2 m) bleached eluvial horizons, and the absence of calcrete.

These six stages were spread over a 675 km$^2$ (that is, approximately 45 km north–south × 15 km east–west) coastal area from south of Jurien Bay to Green Head. The regions were digitized as polygons in a geographic information system (Quantum GIS, http://qgis.org/). All vehicle-accessible roads and tracks from the general area were digitized into the GIS. Randomly positioned points within each of the six distinct dune systems were generated in the GIS, constraining locations between 40 and 200 m from a road or track to facilitate access. Due to the relatively small sizes of vegetation patches within the youngest dune system (that is, stage 1: young mobile dunes), locations were randomly selected without consideration to road or track proximity. Ten plots

per dune system were selected for vegetation surveys, for a total of 60 plots. Plots were selected only in areas that showed no evidence of recent fires (that is, in the last 5 years). The average closest distance between two neighboring plots was 2.1 km. In each plot, we identified an additional seven randomly located 2 m × 2-m subplots. Between June 11 and 16, 2012, seven soil samples (one sample per 2-m × 2-m subplot) were collected in each of the 60 100 m² plots, for a total of 420 samples. Subsampling was done to obtain more accurate estimates of the mean. Samples were taken to 20-cm depth using a 5-cm diameter sand auger, sieved (<2 mm) to remove roots and other large organic debris, and then air dried prior to laboratory analyses (see below).

## Soil Analytical Procedures

Samples from soil profile pits were air dried and analyzed for particle size distribution, pH, carbonate, organic C, total N, total P, and exchangeable cations. Samples from the 60 10 m × 10 m plots were analyzed for total C, total N, total P, sequential P fractionation, micronutrients, carbonate, pH, exchangeable phosphate, extractable N, N mineralization, and exchangeable cations. Soil pH was determined in both deionized water and 10 mM $CaCl_2$ in a 1:2 soil-to-solution ratio using a glass electrode. The concentrations of sand (53 μm–2 mm)-, silt (2 μm–53 μm)-, and clay (<2 μm)-sized particles were determined by the pipette method following pretreatment to remove soluble salts and organic matter (Gee and Or 2002). Total C and N were determined by automated combustion and gas chromatography with thermal conductivity detection using a Thermo Flash 1112 analyzer (CE Elantech, Lakewood, New Jersey). Total P was determined by ignition (550°C, 1 h) and extraction in 1 M $H_2SO_4$ (16 h, 1:50 soil to solution ratio), with phosphate detection by automated neutralization and molybdate colorimetry on a Lachat Quikchem 8500 (Hach Ltd, Loveland, CO). Exchangeable cations were determined by extraction in 0.1 M $BaCl_2$ (2 h, 1:30 soil-to-solution ratio), with detection by inductively coupled plasma optical-emission spectrometry (ICP–OES) on an Optima 7300 DV (Perkin-Elmer Ltd, Shelton, Connecticut) (Hendershot and others 2008). Carbonate content was determined by mass loss after addition of 3 M HCl (Loeppert and Suarez 1996), and organic C was calculated as the difference between total C and carbonate-C. Bulk density was determined by taking three replicate cores of known volume per horizon using a 7.5-cm diam-

eter stainless steel ring and determining the soil mass after drying at 105°C.

Readily exchangeable phosphate was determined by extraction with anion-exchange membranes (AEM) (Turner and Romero 2009). Soil (5 g on a dry-weight basis) was shaken for 24 h with 80 ml deionized water and five anion-exchange resin strips (1 × 4 cm; manufactured by BDH, Poole, UK, and distributed by VWR International, West Chester, Pennsylvania). The strips were rinsed in deionized water and the phosphate recovered by shaking for 1 h in 50 ml of 0.25 M $H_2SO_4$. Phosphate was determined in the acid solution at 880 nm following online neutralization with NaOH by automated molybdate colorimetry using a Lachat Quikchem 8500. Nitrogen was extracted from fresh samples within 8 h of collection. Soil was shaken in 1 M KCl and the solution was filtered through a Whatman No. 42 filter paper. A simple measure of N mineralization was determined by incubation of field-moist soils for 7 days at ambient laboratory temperature and extraction in 1 M KCl, with changes in ammonium and nitrate determined by difference from the corresponding concentrations in fresh soils extracted on the day of collection. Ammonium was determined by automated colorimetry at 660 nm following reaction with phenolate, while nitrate was determined at 520 nm following cadmium-catalyzed reduction to nitrite and reaction with sulfanilamide at pH 8.5. Both ammonium and nitrate were determined using a Lachat Quikchem 8500 flow injection analyzer. Total dissolved N was determined by combustion and gas chromatography on a Shimadzu TOC-TN analyzer, and dissolved organic N was calculated as the difference between the total dissolved N and the sum of ammonium and nitrate. Total exchangeable bases (TEB) was calculated as the sum of Ca, K, Mg, and Na; effective cation-exchange capacity (ECEC) was calculated as the sum of Al, Ca, Fe, K, Mg, Mn, and Na; base saturation was calculated by (TEB ÷ ECEC) × 100. Micronutrients (Cu, Fe, Mn, and Zn) were extracted in Mehlich-III solution (Mehlich 1984) with detection by ICP–OES.

Soil P was fractionated in samples from the 60 10 m × 10 m plots using a modified sequential extraction procedure (Hedley and others 1982). Soils were extracted sequentially with AEM, 0.5 M $NaHCO_3$, 0.1 M NaOH, and 1 M HCl. Residual P was determined on the soil after the four extractions using the ignition and acid-extraction procedure described above. In all cases, extracts were centrifuged (8,000×$g$, 15 min) and decanted for analysis. Each aliquot was neutralized using phe-
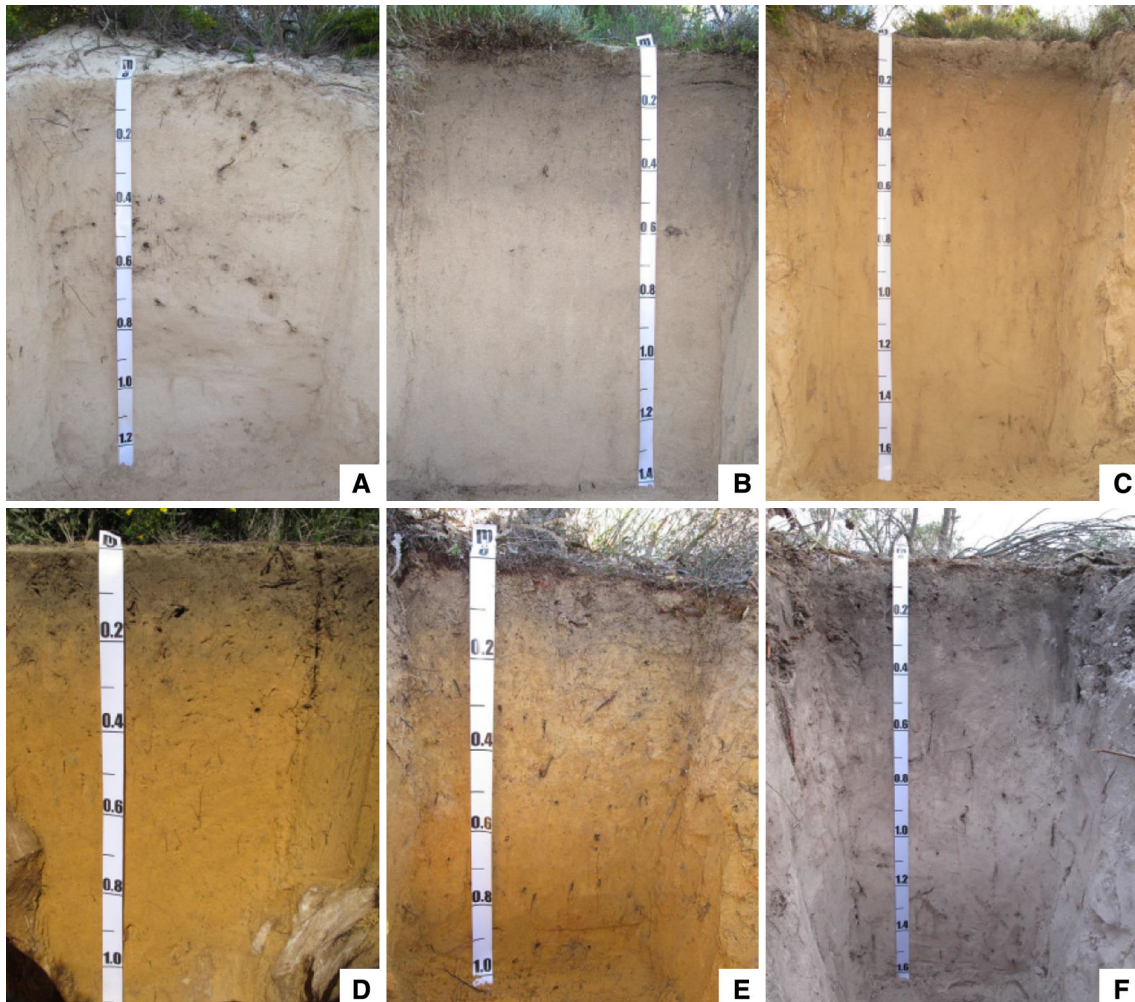
**Figure 2.** Soil development along the Jurien Bay chronosequence. Profiles represent the six main chronosequence stages studied: **A** young Quindalup (<100 years old), **B** medium-aged Quindalup (∼1,000 years old), **C** old Quindalup (∼6,500 years old); **D** young Spearwood (∼120,000 years old), **E** old Spearwood (∼500,000 years old), and **F** Bassendean (>2,000,000 years old). Note the absence of horizon development in the youngest Quindalup profile (**A**), the marked color change in the old Quindalup profile (**C**) as carbonates are removed, the yellow colors indicating residual iron oxides over shallow limestone in the young Spearwood profile (**D**), the incipient eluvial horizon in the old Spearwood profile (**E**), and the complete removal of iron oxides in the Bassendean profile (**F**).

nolphthalein indicator and dilute NaOH or $H_2SO_4$ (as appropriate) and analyzed for inorganic phosphate, and total P. Phosphate was determined by molybdate colorimetry at 880 nm with a 1-cm path length. Total P was determined by the same procedure following acid-persulfate digestion at 80°C overnight in sealed glass tubes. In both cases, standards were prepared in the extract solution following identical neutralization and dilution steps. The detection limit for both procedures was approximately 0.6 mg P $kg^{-1}$ except for resin P (<0.1 mg P $kg^{-1}$). Organic P was calculated as the difference between total P and inorganic phosphate. Fractions were grouped into four pools: organic P (organic P extracted in $NaHCO_3$ and

NaOH), primary mineral P (inorganic P extracted in HCl), non-occluded P (inorganic P extracted in $NaHCO_3$ and NaOH), and occluded P (that is, residual P).

## RESULTS

### Soil Development Along the Jurien Bay Chronosequence

Examples of soil profiles corresponding to the six stages of the Jurien Bay chronosequence are shown in Figure 2, with key diagnostic features and profile-weighted soil properties reported in Table 2. Detailed profile descriptions and full chemical and

physical analyses by genetic horizon are provided in the Online Supplementary Material.

Soils developed on Quindalup dunes (stages 1–3; Figure 2A–C) are light gray-to-grayish brown and exhibit weakly developed surface horizons enriched with organic matter overlying several meters of unweathered calcareous sand. The Quindalup dunes lack diagnostic horizons and are classified as Typic Xeropsamments, reflecting the Xeric moisture regime and sand texture. In the Australian Soil Classification System (Isbell 2002), these soils are Shelly Rudusols. They consist of calcarenites (that is, sand-sized carbonate grains), with up to 82% carbonate in the youngest profile (Table 2). The two youngest dunes qualify as carbonatic (>40% carbonate), but the old Quindalup dunes show evidence of decalcification, with about 25% carbonate throughout the profile. Although much more developed than the younger profiles, the old Quindalup dune does not qualify as an Inceptisol, because the B horizons does not meet all criteria for a cambic horizon. Specifically, although there is evidence of decalcification and a higher color value than underlying horizons, the texture was slightly coarser than very fine sand. All the Quindalup profiles were strongly or very strongly alkaline throughout.

Carbonate in the young Quindalup dunes weathers rapidly and leaches from the profile. Thus, the youngest Spearwood profile (stage 4; Figure 2D) exhibited complete decalcification in the upper horizons, leaving brownish yellow subsoil consisting of greater than 95% residual quartz sand and iron oxide coatings. The yellow color derives from the presence of goethite and weathering of heavy minerals such as ilmenite, garnet, and amphibole (Bastian 1996). The young Spearwood profile (stage 4) contained an undulating indurated petrocalcic horizon (that is, a calcrete cap over the underlying Tamala Limestone), reaching between 40 and 100 cm below the soil surface. The presence of the petrocalcic horizon qualifies the profile as an Inceptisol (Calcic Haploxerepts), consistent with the much older and pedogenically developed nature of the profile. The soil is very friable and has very weak blocky structure.

The depth of sand and depth to limestone in Spearwood dunes increases from west to east, consistent with an increasing degree of weathering and leaching of carbonate. However, we did not encounter limestone in the older Spearwood profile (stage 5; Figure 2E). As a result, the older Spearwood profile classifies as an Entisol (Xeric Quartzipsamment). In the Australian Soil Classification system, the Spearwood profiles are Yellow-Orthic Tenosols, with the younger profile qualifying as a Petrocalcic Great Group. The greater age of the older Spearwood profile was indicated by an incipient eluvial horizon, which becomes much more pronounced in Spearwood profiles further inland (and therefore, presumably older) and at wetter sites further south (Turner and Laliberté, unpublished data). This bleached horizon indicates the early stages of iron oxide removal from the profile as iron–humus complexes and demonstrates that these older Spearwood soils are transitioning toward the final stage of soil development along the chronosequence (stage 6; Figure 2F). Soil pH in water in the Spearwood profiles was neutral and ECEC was less than 2 $cmol_c\ kg^{-1}$. The young and old Spearwood soils along the Jurien Bay chronosequence are broadly equivalent to the yellow and gray phases, respectively, of the Karrakatta sands (McArthur and Bettenay 1974).

The final and oldest stage of the chronosequence (stage 6) is represented by soils developed on the Bassendean dunes (Figure 2). The Bassendean profile is at least 2 million years old (that is, Early Pleistocene) and represents the ultimate end point of pedogenesis along the chronosequence. A thin organic horizon occurs at the surface, consisting of partly decomposed litter and cluster roots from the common nearby trees in the Proteaceae (for example, *Banksia attenuata*, *Banksia menziesii*). The mineral soil is composed entirely of white-to-light gray single grain quartz sand. The sand is completely free of iron oxides, which have been leached from the soil as iron–organic matter complexes. These complexes are often deposited as a spodic horizon (that is, a subsurface accumulation of humus–metal complexes and metal oxides) in the deep subsoil (McArthur 2004), forming a brown iron–humus material known locally as 'coffee rock.' Such soils qualify as Giant Humus Podzols in the Australian Soil Classification (Thompson 1992), but in many cases (for example, Prakongkep and others 2012), they do not qualify as Spodosols in Soil Taxonomy because the spodic horizon is more than 200 cm below the soil surface.

At Jurien Bay, a transition to very pale brown sand, but not a spodic horizon, was encountered at more than 300 cm (further augering was prevented by the water table), although on well-drained areas elsewhere we have encountered spodic materials at several meters depth on Bassendean sands. The nature of the spodic horizon varies markedly depending on proximity to the water table (McArthur and Russell 1978). Despite its great age, the absence of diagnostic features means that the Bassendean profile classifies as an Entisol (Xeric

**Table 2.** Soil Profiles, Approximate Ages, Taxonomic Classes, and Profile-weighted Soil Physical and Chemical Properties for Six Key Stages Along the Jurien Bay Chronosequence, Southwestern Australia

| Chronosequence stage | Approximate age | Soil taxonomy | Pedomorphic features | Carbonate (%) | Sand (%) | Silt (%) | Clay (%) | pH (H$_2$O) | pH (CaCl$_2$) | ECEC (cmol$_c$ kg$^{-1}$) |
|---|---|---|---|---|---|---|---|---|---|---|
| 1 Quindalup young | 100 | Carbonatic, thermic, Typic Xeropsamments | Incipient A horizon | 82 | 98.2 | 1.1 | 0.7 | 9.1 | 8.2 | 12.93 |
| 2 Quindalup medium | 1000 | Carbonatic, thermic, Typic Xeropsamments | Development of A horizon | 66 | 95.9 | 2.1 | 2.0 | 9.2 | 8.1 | 5.52 |
| 3 Quindalup old | 6500 | Siliceous, thermic, Typic Xeropsamments | Moderate decalcification, development of weak structure | 25 | 96.9 | 1.4 | 1.6 | 8.9 | 8.0 | 5.01 |
| 4 Spearwood young | 120,000 (MIS 5e) | Sandy, siliceous, thermic, Calcic Haploxerepts | Decalcification and deposition as an indurated petrocalcic horizon; residual iron oxides throughout the profile | 0 | 94.0 | 2.9 | 3.1 | 6.9 | 6.1 | 1.94 |
| 5 Spearwood old | 480,000 (MIS 13?) | Thermic, Xeric Quartzipsamments | Decalcification; residual iron oxides; incipient eluvial horizon; petrocalcic horizon at considerable depth (if present at all) | 0 | 96.7 | 1.3 | 2.0 | 6.8 | 5.7 | 0.96 |
| 6 Bassendean | > 2,000,000 | Thermic, Xeric Quartzipsamments | Complete removal of iron oxides, leaving residual quartz sand | 0 | 97.3 | 2.3 | 0.3 | 5.6 | 4.4 | 0.98 |

*MIS = marine isotope stage; ECEC = effective cation exchange capacity.*

**Table 3.** Profile-Weighted Nutrient Concentrations for the Upper Meter of Soil in Profile Pits of the Six Main Stages Along the Jurien Bay Chronosequence, Southwestern Australia

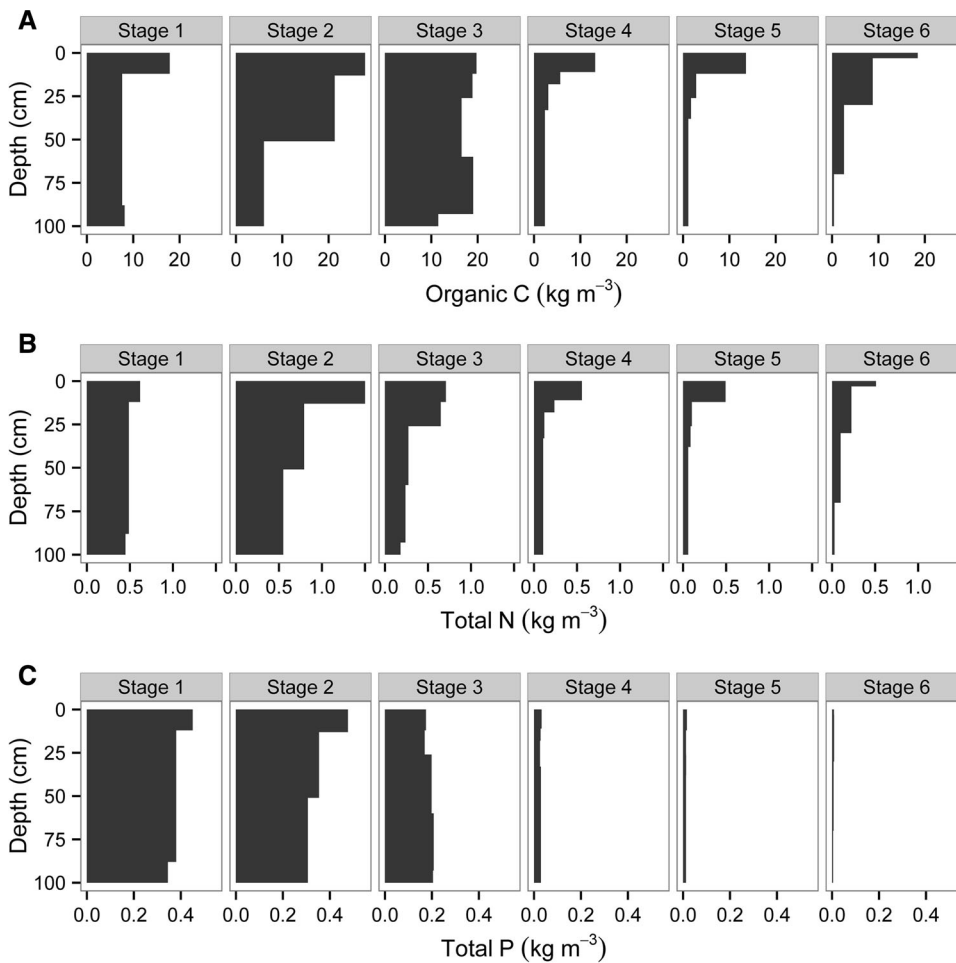| Chronosequence stage | Organic C (g m$^{-2}$) | Total N (g m$^{-2}$) | Total P (g m$^{-2}$) | C:N | C:P | N:P |
|---|---|---|---|---|---|---|
| 1 Quindalup young | 8,900 | 495.5 | 384.3 | 18.0 | 23.2 | 1.3 |
| 2 Quindalup medium | 14,678 | 763.3 | 346.4 | 19.2 | 42.4 | 2.2 |
| 3 Quindalup old | 17,720 | 362.2 | 194.8 | 48.9 | 90.9 | 1.9 |
| 4 Spearwood young | 3,864 | 166.5 | 28.8 | 23.2 | 134.4 | 5.8 |
| 5 Spearwood old | 2,917 | 119.2 | 12.7 | 24.5 | 228.9 | 9.4 |
| 6 Bassendean | 4,063 | 117.8 | 6.4 | 34.5 | 639.2 | 18.5 |



Figure 3. Profile-weighted contents of organic carbon (**A**), total nitrogen (**B**), and total phosphorus (**C**) to one-meter depth along the Jurien Bay chronosequence, southwestern Australia.

Quartzipsamments) in Soil Taxonomy. In the Australian Soil Classification system, the Bassendean profile studied here is a Grey-Orthic Tenosol. The Bassendean soils are equivalent to the Jandakot sands (McArthur and Bettenay 1974), although they appear to lack the spodic horizon around Jurien Bay. Soil pH in water was moderately acid, and ECEC was less than 1 cmol$_c$ kg$^{-1}$.

## Profile-Weighted Organic Carbon, Total Nitrogen, and Total Phosphorus

Organic C in the upper meter of soil increased throughout the Holocene dune sequence (stages 1–3), reaching a maximum of 17.7 kg C m$^{-2}$ in the oldest Quindalup profile (stage 3) (Table 3; Figure 3A). Organic C stocks then declined in
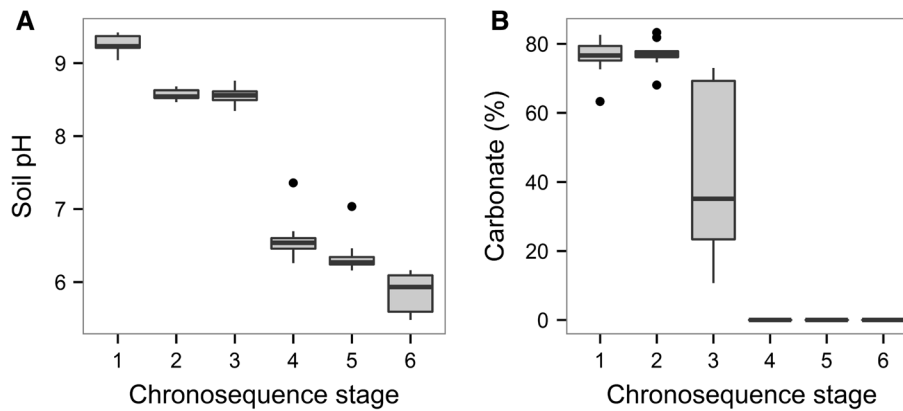
**Figure 4.** Changes in soil pH measured in deionized water (**A**) and carbonate (as $CaCO_3$ equivalent) (**B**) in surface soils along the Jurien Bay chronosequence, southwestern Australia. Values are from ten replicate plots per chronosequence stage. The *central vertical bar in each box* shows the median, the *box* represents the interquartile range, the *whiskers* show the location of the most extreme data points that are still within a factor of 1.5 of the upper or lower quartiles, and the *black points* are values that fall outside the whiskers.

the Spearwood profiles (2.9–3.9 kg C m$^{-2}$), but increased again to 4.1 kg C m$^{-2}$ in the oldest profile (stage 6). Total N (approximating total organic N) followed a slightly different pattern, peaking at 763 g N m$^{-2}$ in the medium-aged Quindalup dune (stage 2), before declining to less than 120 g N m$^{-2}$ in the oldest dunes (Table 3; Figure 3B).

Total P declined continuously along the chronosequence. In the Holocene dunes, total P declined by 50% in about 6500 years, from a maximum of 384 g P m$^{-2}$ in the youngest Quindalup profile (stage 1) to 195 g P m$^{-2}$ in the oldest Quindalup profile (stage 3) (Table 3; Figure 3C). Total P then declined markedly to 28.8 g P m$^{-2}$ in the youngest Spearwood profile and eventually to only 6.4 g P m$^{-2}$ after 2 million years of pedogenesis (stage 6).

Profile-weighted element ratios showed clear patterns expected during long-term pedogenesis (Table 3). The organic C to total N ratio increased in Holocene dunes to a maximum of 48.9 in the old Quindalup profile (stage 3), and then declined in Spearwood dunes, although the ratio increased to 34.5 in the oldest profile (stage 6). The organic C to total P ratio increased continuously throughout the sequence, from a low of 23.2 in the youngest Holocene dune (stage 1) to a maximum of 639 in the oldest profile on Bassendean Sand (stage 6). Similarly, the profile-weighted N:P increased from 2.2 or less in the Holocene dunes to 18.5 in the oldest profile (stage 6).

## Changes in pH and Carbonate in Surface Soils

Soil pH in water declined from very strongly alkaline (pH 9.2) in the youngest dunes to strongly alkaline (pH 8.6) in older Quindalup dunes, and then to moderately acid (pH 5.9) in the Bassendean soil (Figure 4A). Soil pH in 10 mM $CaCl_2$ followed a similar pattern but approximately one pH unit lower, with values decreasing from 8.2 in the youngest dunes to 4.8 in the oldest dunes. Carbonate in surface soils was 76–78% in the youngest two dunes, declining to 43% in the older Quindalup dunes, although values for old dunes varied markedly among replicate plots (Figure 4B). No carbonate was detected in Spearwood or Bassendean dunes.

## Changes in Carbon, Nitrogen, and Phosphorus in Surface Soils

Organic C concentrations in surface soils increased initially to a maximum of 18.8 g C kg$^{-1}$ in the medium-aged Quindalup dunes (stage 2) and then declined to less than 7 g C kg$^{-1}$ on Spearwood and Bassendean dunes (stages 4–6; Figure 5A). Total N followed a similar pattern, increasing to 1.17 g N kg$^{-1}$ in the medium-aged Quindalup dunes and declining to 0.30 g N kg$^{-1}$ or less in the older stages (Figure 5B). Total P increased initially from 350 mg P kg$^{-1}$ on the youngest dunes (stage 1) to 433 mg P kg$^{-1}$ on the medium-aged Quindalup
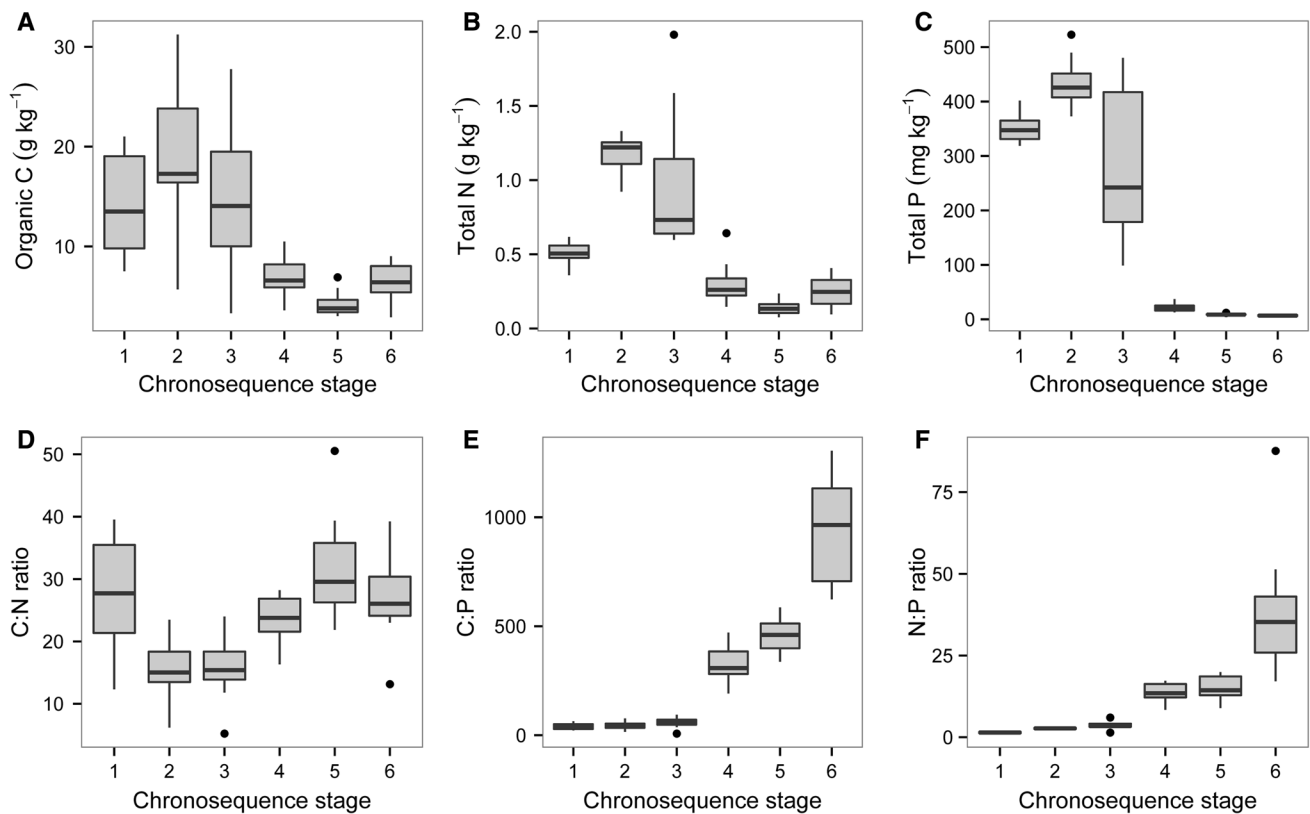
**Figure 5.** Concentrations of organic carbon (**A**), total nitrogen (**B**), total phosphorus (**C**), and their ratios (**D–F**) in surface soils along the Jurien Bay chronosequence, southwestern Australia. *Values* are from ten replicate plots per chronosequence stage. See legend to Figure 4 for an explanation of the box plots.

dunes (stage 2; Figure 5C), reflecting redistribution of P in surface horizons by plants (Figure 3). It then declined to 21.5 mg P kg$^{-1}$ on the Spearwood dunes and then to 6.7 mg P kg$^{-1}$ on the Bassendean dunes (stage 6; Figure 5C).

The organic C to total N ratio in surface soil declined initially from 27.0 in the youngest soils to about 15.5 in older Quindalup soils, and then increased to a maximum of 31.6 in old Spearwood soils (Figure 5D). Organic C to total P ratios increased markedly from very low values in Quindalup soils ( ≤ 51 on stages 1–3) to around 1,000 in the oldest dunes (Figure 5E). The total N:P ratio followed a similar pattern to the organic C:P ratio, increasing consistently from very low values on young soils (<4 on young Quindalup dunes) to maximum values (41.6) on the oldest soils (Bassendean dunes; stage 6) (Figure 5F).

## Phosphorus Fractionation in Surface Mineral Soils

Phosphorus fractions determined by sequential extraction closely followed the classic Walker and

Syers (1976) model of P transformations during pedogenesis (Figure 6). The youngest soils (stages 1–3) were dominated by HCl-extractable phosphate, which occurred at up to 355 mg P kg$^{-1}$ (Figure 6A) and accounted for up to 90% of the total P (Figure 6B). The HCl-extractable phosphate pool declined to low concentrations (<1 mg P kg$^{-1}$) in Spearwood and Bassendean soils (stages 4–6). The majority of the remainder of the total P in the Quindalup dunes was present as non-occluded inorganic phosphate, which occurred at up to 35.7 mg P kg$^{-1}$ and accounted for 4–8% of the total P. Non-occluded inorganic phosphate (that is, bicarbonate plus NaOH-extractable inorganic phosphate) declined to low concentrations (<1 mg P kg$^{-1}$) in older soils, but still represented 11–23% of the total P. Occluded P (that is, residual P) occurred at relatively minor concentrations throughout the sequence (up to 29.2 mg P kg$^{-1}$ in the oldest Quindalup dunes; stage 3), but accounted for a much greater proportion of the total P in older soils (29–50%) than on younger soils (2–17%). The decline in the proportion of occluded P in the oldest soils appears to be related to the increasing relative
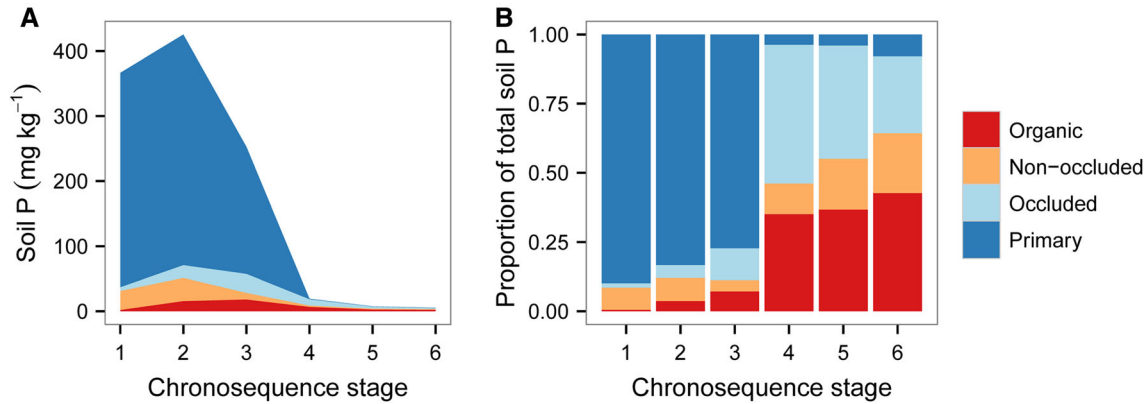
**Figure 6.** Phosphorus fractionation by sequential extraction in surface soils along the Jurien Bay chronosequence, southwestern Australia, including concentrations (**A**) and proportions of the total phosphorus (**B**). Phosphorus is grouped into primary mineral phosphate (extracted in HCl), organic phosphorus (organic phosphorus extracted in NaHCO₃ and NaOH), non-occluded phosphorus (inorganic phosphate extracted in NaHCO₃ and NaOH), and occluded phosphorus (that is, residual phosphorus not extracted in any step). *Values* are the means of ten replicate plots per chronosequence stage.

importance of organic P under conditions of extremely low soil P. Organic P was only 2 mg P kg⁻¹ in the youngest soil, increased to the maximum concentration in the oldest Quindalup soil (18.2 mg P kg⁻¹; stage 3), and then declined to low concentrations in Spearwood and Bassendean soils (<3 mg P kg⁻¹; stages 4–6). However, organic P increased continuously as a proportion of the total P throughout the sequence, reaching 40% in the Bassendean soil (stage 6). Total P calculated from the sum of sequential fractions corresponded closely with total P values determined independently by ignition and acid extraction (Figure 5C). The relationship when forced through the origin was described by the equation $Y = 1.03x$ ($R^2 = 0.98$, $P < 0.0001$), where $Y$ = total P determined by ignition and $x$ = total P by sequential fractionation.

## Extractable Phosphorus and Nitrogen in Surface Mineral Soils

Phosphate extracted by AEM was greatest in the medium-aged Quindalup dunes (2.1 mg P kg⁻¹; stage 2) and then declined to very low values on the two oldest stages (≤ 0.5 mg P kg⁻¹) (Figure 7A). Extractable N followed a similar pattern (Figure 7B). Total dissolved N increased to maximum values on the medium-aged Quindalup dunes (stage 2) and then declined to lower values on older soils. Dissolved organic N accounted for the majority of the total dissolved N, being approximately 20 mg N kg⁻¹ in medium and older Quindalup dunes and no more than 10 mg N kg⁻¹ elsewhere. Both extractable ammonium and nitrate increased from the lowest values in the young

Quindalup dunes (stage 1) to maximum values in the medium-aged Quindalup dunes (stage 2), and then declined to moderate values on older soils (Figure 7B). Ammonium concentrations declined following soil incubation, with losses mirroring concentrations of extractable ammonium (that is, greatest in the medium-aged Quindalup dunes). Nitrate mineralization was greatest in medium and old Quindalup dunes (0.3–0.5 mg N kg⁻¹ day⁻¹), with negligible mineralization on the youngest and oldest dunes (Figure 7C).

## Exchangeable Cations in Surface Soils

Extractable Al concentrations were no more than 0.01 cmol_c kg⁻¹ along the entire sequence, so ECEC was dominated throughout by base cations (Figure 7D), with base saturation around 100%. Effective cation exchange capacity was the greatest in the youngest Quindalup soils (24.9 cmol_c kg⁻¹; stage 1), declining by about 50% in older Quindalup dunes (stages 2–3) and then further to very low values in the older soils (a minimum value of 2.0 cmol_c kg⁻¹ in old Spearwood soils; stage 5) (Figure 7D).

The exchange capacity was dominated by calcium throughout the sequence, with maximum values on the youngest Quindalup dunes (23.0 cmol_c kg⁻¹) and minimum values on the oldest two stages (<2.0 cmol_c kg⁻¹; stages 5–6). Exchangeable magnesium declined from 1.81 cmol_c kg⁻¹ in the youngest soil to 0.33 cmol_c kg⁻¹ in old Spearwood soils (Figure 7D). Exchangeable potassium concentrations were much lower, with very low values (∼0.01 cmol_c kg⁻¹) on the
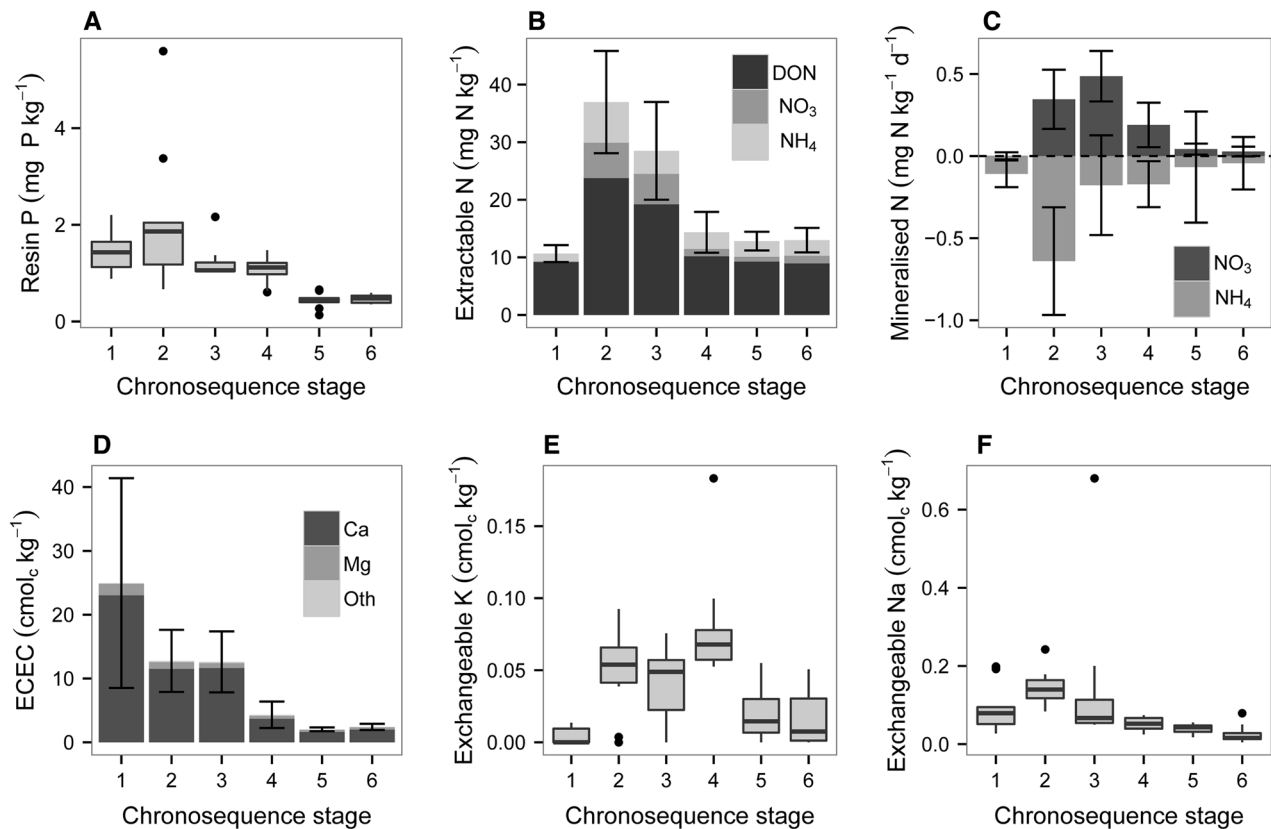
**Figure 7.** Extractable (readily bioavailable) nutrient concentrations in surface soils along the Jurien Bay chronosequence, southwestern Australia, showing anion-exchange membrane extractable phosphate (**A**), KCl-extractable nitrogen (**B**), mineralized nitrogen (**C**), effective cation-exchange capacity (ECEC) and the contribution of calcium, magnesium, and other cations (**D**), exchangeable potassium (**E**), and exchangeable sodium (**F**). *Values* are the mean ($\pm 1$ standard deviation) of ten replicate plots per chronosequence stage. See legend to Figure 4 for an explanation of the box plots.

youngest soils, increasing to about 0.05 $\text{cmol}_c$ $\text{kg}^{-1}$ on older Quindalup and young Spearwood soils (stages 3–4), and then declining to low values (0.02 $\text{cmol}_c$ $\text{kg}^{-1}$) in the two oldest soils (stages 5–6; Figure 7E). Exchangeable sodium followed a similar pattern, with maximum values in the medium-aged Quindalup dunes ($\sim 0.15$ $\text{cmol}_c$ $\text{kg}^{-1}$) and declining to low values (0.03 $\text{cmol}_c$ $\text{kg}^{-1}$) on Bassendean dunes (Figure 7F).

## Micronutrient Concentrations in Surface Mineral Soils

Of the four micronutrients measured, copper concentrations were extremely low throughout the sequence relative to the amounts considered adequate for crops, while manganese and zinc were moderately low, and iron moderate to adequate (for example, Lindsay and Norvell 1978; Adriano 1986) (Figure 8). Mehlich-III extractable copper

concentrations were the lowest in the youngest Quindalup dunes (stage 1; 0.011 mg Cu $\text{kg}^{-1}$) and greatest in the youngest Spearwood dunes (stage 4; 0.043 mg Cu $\text{kg}^{-1}$). Copper concentrations were lowest, however, on the old Spearwood dunes (stage 5; 0.008 mg Cu $\text{kg}^{-1}$). Mehlich-III extractable iron concentrations were low in the Holocene dunes (stages 1–3; $<3$ mg Fe $\text{kg}^{-1}$) but much greater in the older dunes (25–39 mg Fe $\text{kg}^{-1}$). Mehlich-III extractable manganese concentrations followed a similar pattern to copper, increasing from the lowest values on the youngest Quindalup dunes (mean 0.71 mg Mn $\text{kg}^{-1}$) to the greatest concentrations on young Spearwood dunes (stage 4; 3.01 mg Mn $\text{kg}^{-1}$). Mehlich-III extractable zinc concentrations were greatest in the youngest Quindalup dunes (stage 1; 1.43 mg Zn $\text{kg}^{-1}$) but changed little along the sequence. The lowest zinc concentrations were detected in the Bassendean dunes (stage 6; 0.54 mg Zn $\text{kg}^{-1}$).
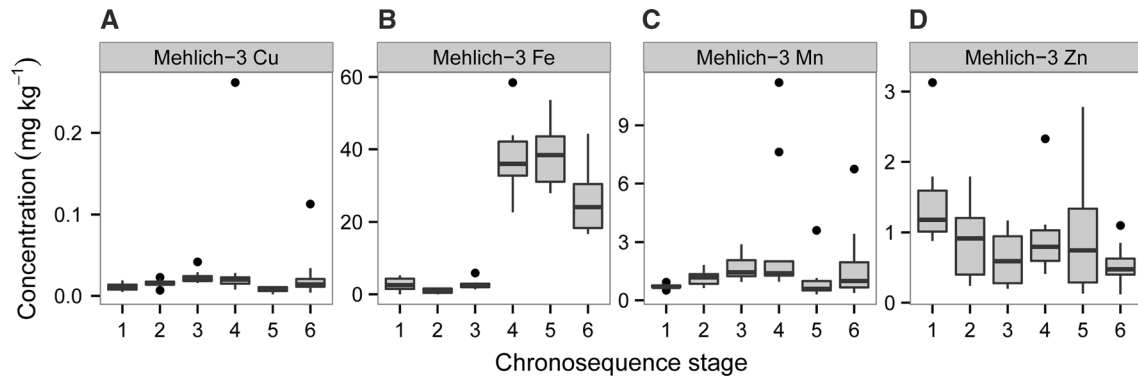
**Figure 8.** Concentrations of extractable micronutrients in surface soils along the Jurien Bay chronosequence, southwestern Australia, including copper (**A**), iron (**B**), manganese (**C**), and zinc (**D**). *Values* are from ten replicate plots per chronosequence stage. See legend to Figure 4 for an explanation of the box plots.

## DISCUSSION

### Pedogenesis Along the Jurien Bay Chronosequence

Soil development along the Jurien Bay chronosequence is consistent with previous detailed studies in the Perth region that have shown a clear west-to-east increase in weathering and soil development (Bastian 1996; McArthur 2004). Soils with ages between the oldest Quindalup and youngest Spearwood dunes, a span of many thousands of years, are not found along the sequence because they have been buried by younger Holocene sediments or submerged beneath present sea level (Brooke and others 2014). However, the Quindalup and Spearwood successions, coupled with the oldest Bassendean soil, are sufficient to reconstruct the transition from calcareous sands to siliceous quartz sands over 2 million years of pedogenesis.

Young soils are strongly alkaline, but undergo relatively rapid acidification and leaching of carbonate. The carbonate precipitates at depth to form a calcrete cap overlying the Tamala Limestone, leaving an overlying layer of residual quartz sand. With further pedogenesis, the calcite is progressively leached away and residual iron oxides are leached from the profile, leaving bleached quartz grains. Depending on landscape position, the iron oxides can form a spodic horizon consisting of iron–humus complexes that may be many meters below the soil surface. Although the leaching of iron oxides is not pronounced along the Jurien Bay chronosequence, an incipient eluvial horizon was evident in profile pits on the most easterly Spearwood dunes, and we have studied eluvial horizons up to 2-m deep in old Spearwood dunes under greater rainfall further south.

### Patterns of Soil Nutrients Along the Chronosequence

Despite the modest rainfall under a Mediterranean climate at Jurien Bay, changes in C, N, and P along the chronosequence were remarkably consistent with expectations of the Walker and Syers (1976) model of nutrient transformations during pedogenesis. Profile weights of organic C and N increased rapidly in the early stages of pedogenesis and then declined. In contrast, total P declined continuously throughout the chronosequence, reaching extremely low levels on the oldest dunes. Indeed, total P concentrations in Bassendean soils are among the lowest reported globally. In parallel, profile-weighted C:P and N:P ratios increased continuously along the sequence, reinforcing the expectation of strengthening P limitation in old soils (see below) (Laliberté and others 2012; Hayes and others 2014). Changes in soil P chemistry determined by sequential fractionation were also in accordance with the Walker and Syers (1976) model, with a marked decline in primary mineral P during the early stages of pedogenesis and increasing importance of organic and occluded P in old soils. The exception was the decline in the proportion of occluded P in the oldest soils, which appears to be due to the increasing importance of organic P in those soils. This pattern of P transformations during pedogenesis has been observed consistently in chronosequences around the world under a variety of climates and in soils developed on markedly different parent materials (Walker and Syers 1976; Crews and others 1995; Peltzer and others 2010; Selmants and Hart 2010; Turner and others 2012; Izquierdo and others 2013).

To assess changes in soil fertility along the sequence over a much broader area than possible through soil profile pits, we determined concentrations of total and available nutrients in 100 m$^2$ plots distributed along the six key chronosequence stages. These samples further supported expectations of changes in nutrient availability and limitation along the chronosequence (Laliberté and others 2012; Hayes and others 2014). For example, measures of N availability increased initially and then declined, as did some cations (that is, potassium and sodium) and micronutrients, whereas extractable P, exchangeable calcium and magnesium, and extractable zinc declined continuously along the sequence. The latter is somewhat surprising given evidence for zinc limitation on the youngest soils (Laliberté and others 2012), including the high resorption efficiency for zinc in leaves of native plants (Hayes and others 2014). This result suggests that high pH, rather than low zinc concentrations, is the cause of apparent zinc limitation due to the slow diffusion of zinc in calcareous soils (Melton and others 1973).

Copper deficiency is widespread on strongly weathered soils of Western Australia, including on acid and calcareous sands (Holloway and others 2008), and the extremely low copper concentrations throughout the Jurien Bay chronosequence are reflected in foliar copper concentrations far below those considered adequate for crop growth (Hayes and others 2014). Copper availability therefore represents a potentially important micronutrient constraint to plant performance throughout the Jurien Bay chronosequence, although we did not observe strong responses to micronutrients on most soils in a previous phytometer experiment (Laliberté and others 2012), or high copper resorption in the leaves of native plants (Hayes and others 2014). However, the limited resorption might be explained by the fact that plants with low foliar copper concentrations tend to show low copper resorption efficiency from leaves, because a greater proportion of the copper is firmly bound in structural constituents such as cell walls (White 2012).

## Comparison with Other Long-Term Chronosequences

The Jurien Bay chronosequence differs from previously studied long-term chronosequences in a number of important ways, including its carbonate parent material, Mediterranean climate, and species-rich shrubland vegetation. In terms of climate, there are only two long-term chronosequences under dry climates with which to compare the Jurien Bay chronosequence. In the Northern Arizona Volcanic Field, a 3 million-year chronosequence on basalt under 340-mm annual rainfall and 11°C mean annual temperature, total P in surface soil declined by 60% during the lifetime of the sequence (Selmants and Hart 2010). Primary mineral P in surface soils declined by 75%, but was still abundant (35% of the total P) in the oldest soils. However, non-occluded P declined to low concentrations and organic P increased continuously throughout the sequence, although it only accounted for 8% of the total P on the oldest soils.

In contrast, primary mineral P in apatite declined almost completely after ca 100,000 years of pedogenesis after a 3 million-year chronosequence of alluvial terraces supporting Californian grassland under 300 mm annual rainfall and 16°C mean annual temperature (Baisden and others 2002). We interpret the differences in the depletion of primary mineral P between these two western USA sequences, despite similar rainfall, as an indication of the importance of parent material in determining long-term rates of P transformations, although this does not account for possible differences in paleoclimate. Although total P and other P forms were not reported for the San Joaquin terrace sequence, it appears to most closely resemble rates of P depletion along the Jurien Bay chronosequence, where primary mineral phosphate was completely leached from the soil within 120,000 years. However, all three of these relatively dry chronosequences appear to conform to the Walker and Syers (1976) model of P transformations during pedogenesis, although the rates of P transformations are considerably slower than under more humid climates.

The Jurien Bay chronosequence is comparable in some ways to the long-term coastal dune chronosequence at Cooloola in eastern Australia (Thompson 1981; Walker and others 1981). Although the dates of dune formation at Cooloola are poorly constrained, the chronosequence spans approximately 700,000 years of pedogenesis, and it seems likely that at least some of the dune systems correspond in age to those at Jurien Bay. For example, thermal luminescence dating gives an age of 120,000 years for dune stage 5 at Cooloola (Tejan-Kella and others 1990). The Cooloola sequence differs from Jurien Bay because it is in a humid subtropical climate (1,500 mm of rainfall per year, mostly falling in the summer) and the parent material contains little carbonate (Thompson 1981). As a consequence, initial total soil P concentrations are much lower at Cooloola than at

Jurien Bay: young vegetated dunes at Cooloola contain less than 30 g P m$^{-2}$ (Thompson 1981; B.L. Turner, unpublished data), equivalent to the Jurien Bay chronosequence after 120,000 years of pedogenesis (Table 3). However, despite the absence of carbonate, soil development at Cooloola is qualitatively similar to that at Jurien Bay, with leaching of iron oxide coatings on quartz grains leaving bleached quartz profiles at least 2 m deep after approximately 200,000 years of pedogenesis. Eventually, after 400,000 years, the spodic horizon occurs up to 20 m below the soil surface above a profile of clean quartz sand (Thompson 1981, 1992), forming Giant Humus Podzols. This process therefore occurs more rapidly than at Jurien Bay, which is consistent with the greater productivity (with tall eucalypt forest) and rainfall falling in the warmest part of the year at Cooloola.

Most coastal dune chronosequences involve the development of podzols, in which P depletion occurs in parallel with the leaching of iron and aluminum from the upper part of the soil profile. Stevens and Walker (1970) and Jenny (1941) summarized a series of early studies of sand dune chronosequences from Sweden, England, and elsewhere. These and more recent studies of young coastal dune sequences provide support for the importance of rainfall in terms of podzol development and P depletion (Syers and others 1970; Lichter 1998; Tackett and Craft 2010). This is demonstrated clearly by comparison of the Jurien Bay chronosequence with Holocene coastal dune systems under a perhumid climate along the west coast of the South Island of New Zealand (Wells and Goff 2007). These sequences began to form approximately 6500 years before present and therefore span the same time period as the Quindalup dune system at Jurien Bay. However, dune formation on the west coast of New Zealand is triggered by earthquakes along the Alpine Fault, which causes landslides and sediment transport to the ocean and subsequent dune formation. A well-studied example occurs under temperate rainforest at Haast (Turner and others 2012). Although total P in young dunes at Haast is similar to young dunes at Jurien Bay (300–400 mg P kg$^{-1}$), rainfall is much higher at Haast (3,500 mm year$^{-1}$), so the rate of P depletion is correspondingly greater. Comparing concentrations in the upper mineral soil, total P increased initially at Jurien Bay (through concentration of P in topsoil by plants) and then declined to around 200 mg P kg$^{-1}$ after 6500 years. At Haast, total P declined rapidly from about 320 mg P kg$^{-1}$ initially to about 200 mg P kg$^{-1}$ in just a few hundred years, and then to about 100 mg P kg$^{-1}$ after

about 4000 years. At that point, the majority of the total soil P at Haast is in organic forms ($>80\%$) compared to about 10% at Jurien Bay, in agreement with expectations for the influence of rainfall on soil P composition (Walker and Syers 1976; Vitousek 2004). However, differences in vegetation are also likely to be important, because the conifers that are abundant in the early stages of the Haast chronosequence produce leaf litter that decomposes slowly, acidifies the soil rapidly, and promotes the formation of thick organic horizons within a few hundred years (Coomes and Bellingham 2011; Turner and others 2012).

The rate of decline of soil P at Haast is similar to that at the nearby Franz Josef post-glacial chronosequence, when the loss rate is expressed as a proportion of the total P (Turner and others 2012). Although these two sequences differ in their parent material, they have formed under similar vegetation and climate. It is therefore surprising that the proportional rate of total P decline at Franz Josef is similar to that at Jurien Bay, despite large differences in parent material and climate (the Franz Josef sequence is developed in graywacke and schist deposits under 3,500–6,000-mm annual rainfall). At Jurien Bay, total profile P to 1 m declined from 384 to 28.8 g P m$^{-2}$ in 120,000 years (that is, the young Spearwood dunes), leaving 7.5% of the original P remaining. At Franz Josef, total P in the upper 75 cm, including stones, declined from 1,292 g m$^{-2}$ initially to 76 g P m$^{-2}$ after 120,000 years, leaving 5.9% of the total P remaining (Walker and Syers 1976). This provides further support for the suggestion that a consistent pattern of proportional loss of P occurs among chronosequences (Turner and others 2012).

## Fire and Soil Nutrient Dynamics During Ecosystem Development

Fire is an important driver of ecosystem nutrient status, with implications for the rate of nutrient transformations during pedogenesis (Peltzer and others 2010). Fire causes the loss of N in gaseous forms by volatilization from vegetation, litter, and surface soil, but mineralizes organic P in live and dead vegetation and returns it to the soil in inorganic form (Carter and Darwin 2004; Certini 2005). These processes act against the long-term pedogenic trend of increasing N and declining P, and therefore effectively set the ecosystem back to an earlier state in terms of soil nutrient stocks. It might therefore be expected that systems in which fire is a major and frequent disturbance, such as the kwongan of southwestern Australia, would experience a

slower rate of ecosystem development than less fire-prone systems, perhaps even to the extent that the long-term steady state P concentration is greater in more fire-prone systems than in comparable areas that rarely experience fire. For example, fires on Swedish Islands are of sufficient intensity to burn peat, which maintains P availability and prevents the onset of retrogression on the larger islands that burn frequently, compared to small islands that almost never experience fire (Wardle and others 2004). Fires are a common disturbance along the Jurien Bay chronosequence, but clearly this has not prevented the ecosystem progressing toward extremely low P availability, even on relatively young (that is, 120,000 year) soils. This might be because fire promotes P loss in this ecosystem, either as wind-blown ash, or when rainfall onto burnt areas causes the released P (and N) to be transported downslope in surface runoff or in leachate through these sandy soils (Carter and Darwin 2004; Certini 2005).

## Ecological Consequences of Pedogenic Change Along the Jurien Bay Chronosequence

Pedogenesis and the associated changes in nutrient status described here have important implications for plant and microbial communities along the Jurien Bay chronosequence. In particular, the results presented here provide further support for experimental evidence suggesting that potential nutrient limitation of plant growth along the chronosequence corresponds closely to expectations of the Walker and Syers (1976) model, with N limitation on young soils (perhaps along with other nutrients such as potassium), co-limitation by multiple nutrients on intermediate aged soils, and strong P limitation on old soils (Laliberté and others 2012). This pattern is supported by evidence from foliar nutrient analysis, with remarkably strong community-wide declines in foliar P from young to old soils, with concentrations spanning virtually the global range of foliar P (0.1–3.0 mg P g$^{-1}$ at Jurien Bay) (Hayes and others 2014). In addition, there is a marked increase in foliar N:P ratios along the sequence (from 8 on young soils to 42 on oldest soils) and a parallel increase in foliar P resorption efficiency from zero to 79%, with all species converging on an extremely conservative P use strategy on the oldest soils (Hayes and others 2014). Some Proteaceae, which become particularly abundant on the oldest soils, express a number of adaptations to acquire and conserve P, including the formation of cluster roots (Lambers and others

2006), extremely high P use efficiency (Denton and others 2007), low levels of protein and ribosomal RNA (Sulpice and others 2014), and the replacement of phospholipids by sulfolipids and galactolipids during leaf development (Lambers and others 2012). Of particular interest is that plant diversity increases continuously along the chronosequence as soils age (Laliberté and others 2013a, 2014). This conforms to a pattern observed previously in other long-term soil chronosequences (Wardle and others 2008), and primarily reflects the fact that plant species pools (that is, sets of species from the regional flora that can successfully grow in a given habitat) on older acidic and P-impoverished soils along the chronosequence are much larger than those from younger alkaline soils (Laliberté and others 2014). The species-rich flora in the Jurien Bay region therefore provides an important opportunity to study the influence of nutrient availability and limitation on plant diversity and distribution in a Mediterranean climate (Laliberté and others 2013a, 2014).

## CONCLUSIONS

Soil development along coastal dune systems under a Mediterranean climate in southwestern Australia involves acidification and leaching of carbonate, accumulation of organic matter, and a continual decline in total P. Patterns of nutrient concentrations correspond remarkably well with the Walker and Syers (1976) model of nutrient transformations and limitation during ecosystem development, with a number of lines of evidence pointing to N limitation on young soils (with possible micronutrient limitation), co-limitation by N and P on the intermediate-aged soils, and strong P limitation on old soils. Indeed, total P concentrations reach extremely low levels in the oldest soils and plant communities demonstrate abundant signs of adaptation to P stress (Hayes and others 2014). The Jurien Bay chronosequence therefore represents an important example of long-term pedogenesis and associated changes in nutrient availability and limitation in a Mediterranean climate. The species-rich nature of the regional plant community offers the possibility of linking the long-term consequences of soil development and associated shifts in nutrient availability and stoichiometry to patterns of plant species distribution and diversity.

## ONLINE SUPPLEMENTARY MATERIAL

Two online supplementary files contain (1) descriptions of profiles corresponding to the six

stages along the Jurien Bay chronosequence, and (2) a table of physical and chemical data on soil profiles by genetic horizon, including particle size analysis, total carbon, nitrogen, and phosphorus, carbonate, pH, and exchangeable cations. Data on surface soils in the sixty 10 m × 10 m plots are available on request.

## ACKNOWLEDGMENTS

## REFERENCES

Adriano DC. 1986. Trace elements in the terrestrial environment. New York: Springer.

Baisden WT, Amundson R, Brenner DL, Cook AC, Kendall C, Harden J. 2002. A multi-isotope C and N modeling analysis of soil organic matter turnover and transport as a function of soil depth in a California annual grassland soil chronosequence. Glob Biogeochem Cycles 16:1135. doi:10.1029/2001GB001823.

Barrows TT, Juggins S. 2005. Sea-surface temperatures around the Australian margin and Indian Ocean during the Last Glacial Maximum. Quat Sci Rev 24:1017–47.

Bastian LV. 1996. Residual soil mineralogy and dune subdivision, Swan Coastal Plain, Western Australia. Aust J Earth Sci 43:31–44.

Beard JS. 1984. Biogeography of the kwongan. In: Pate JS, Beard JS, Eds. Kwongan: plant life of the sandplain. Nedlands: University of Western Australia Press. p 1–26.

Bell DT, Hopkins AJM, Pate JS. 1984. Fire in the kwongan. In: Pate JS, Beard JS, Eds. Kwongan: plant life of the sandplain. Nedlands: University of Western Australia Press. p 178–204.

Bell DT, Plummer JA, Taylor SK. 1993. Seed germination ecology in southwestern Western Australia. Bot Rev 59:24–73.

Berger WH. 2008. Sea level in the late Quaternary: patterns of variation and implications. Int J Earth Sci 97:1143–50.

Brooke BP, Olley JM, Pietsch T, Playford PE, Haines PW, Murray-Wallace CV, Woodroffe CD. 2014. Chronology of Quaternary coastal aeolianite deposition and the drowned shorelines of southwestern Western Australia—a reappraisal. Quat Sci Rev 93:106–24.

Burges A, Drover D. 1953. The rate of podzol development in sands of the Woy Woy District, NSW. Aust J Bot 1:83–94.

Carter MC, Darwin Foster C. 2004. Prescribed burning and productivity in southern pine forests: a review. For Ecol Manag 191:93–109.

Certini G. 2005. Effects of fire on properties of forest soils: a review. Oecologia 143:1–10.

Coomes DA, Bellingham PJ. 2011. Temperate and tropical podocarps: how ecologically alike are they? In: Turner BL, Cernusak LA, Eds. Ecology of the Podocarpaceae in tropical forests. Smithsonian Contributions to Botany. Washington, DC: Smithsonian Institution Scholarly Press. p 119–40.

Coomes D, Bentley W, Tanentzap A, Burrows L. 2013. Soil drainage and phosphorus depletion contribute to retrogressive succession along a New Zealand chronosequence. Plant Soil 367:77–91.

Crews TE, Kitayama K, Fownes JH, Riley RH, Herbert DA, Mueller-Dombois D, Vitousek PM. 1995. Changes in soil phosphorus fractions and ecosystem dynamics across a long chronosequence in Hawaii. Ecology 76:1407–24.

Denton M, Veneklaas EJ, Freimoser F, Lambers H. 2007. *Banksia* species (Proteaceae) from severely phosphorus-impoverished soils exhibit extreme efficiency in the use and re-mobilization of phosphorus. Plant Cell Environ 30:1557–65.

Dodson JR. 2001. Holocene vegetation change in the mediterranean-type climate regions of Australia. Holocene 11:673–80.

Enright NJ, Lamont BB, Miller BP. 2005. Anomalies in grasstree fire history reconstructions for south-western Australian vegetation. Austral Ecol 30:668–73.

Fujioka T, Chappell J, Fifield LK, Rhodes EJ. 2009. Australian desert dune fields initiated with Pliocene-Pleistocene global climatic shift. Geology 37:51–4.

Gee GW, Or D. 2002. Particle size analysis. In: Dane JH, Topp C, Eds. Methods of soil analysis, Part 4—Physical methods. Madison: Soil Science Society of America. p 255–93.

Geological Survey of Western Australia. 1990. Geology and Mineral Resources of Western Australia. Perth: Western Australian Geological Survey. p 827.

Glassford DK, Killigrew LP. 1976. Evidence for Quaternary westward extension of the Australian desert into south-western Australia. Search 7:394–6.

Griffin EA, Burbidge AA. 1990. Description of the region. In: Burbidge AA, Hopper DS, van Leeuwen S, Eds. Nature conservation, landscape and recreation values of the Lesueur area. Perth: Environmental Protection Authority. p 15–24.

Harden JW. 1982. A quantitative index of soil development from field descriptions: example from a chronosequence in central California. Geoderma 28:1–28.

Hayes P, Turner BL, Lambers H, Laliberté E. 2014. Foliar nutrient concentrations and resorption efficiency in plants of contrasting nutrient-acquisition strategies along a 2-million-year dune chronosequence. J Ecol 102:396–410.

Hearty PJ, O'Leary MJ. 2008. Carbonate eolianites, quartz sands, and Quaternary sea-level cycles, Western Australia: a chronostratigraphic approach. Quat Geochronol 3:26–55.

Hedley MJ, Stewart JWB, Chauhan BS. 1982. Changes in inorganic and organic soil phosphorus fractions induced by cultivation practices and by laboratory incubations. Soil Sci Soc Am J 46:970–6.

Hendershot WH, Lalande H, Duquette M. 2008. Chapter 18. Ion exchange and exchangeable cations. In: Carter MR, Gregorich E, Eds. Soil sampling and methods of analysis. Boca Raton: Canadian Society of Soil Science and CRC Press. p 173–8.

Hewgill FR, Kendrick GW, Webb RJ, Wyrwoll KH. 1983. Routine ESR dating of emergent Pleistocene marine units in Western Australia. Search 14:215–17.

B. L. Turner and E. Laliberté

Holloway RE, Graham RD, Stacey SP. 2008. Micronutrient deficiencies in Australian field crops. In: Alloway BJ, Ed. Micronutirent deficiencies in global crop production. Berlin: Springer. p 63–92.

Hopper SD. 2014. Sandplain and kwongan: historical spellings, meanings, synonyms, geography and definition. In: Lambers H, Ed. Plant life on the sandplains in Southwest Australia, a global biodiversity hotspot. Crawley: University of Western Australia Publishing.

Hopper SD, Gioia P. 2004. The Southwest Australian Floristic Region: evolution and conservation of a global hot spot of biodiversity. Annu Rev Ecol Evol Syst 35:623–50.

Huggett RJ. 1998. Soil chronosequences, soil development, and soil evolution: a critical review. Catena 32:155–72.

Isbell RF. 2002. The Australian soil classification. revised edn. Collingwood: CSIRO Publishing.

Izquierdo JE, Houlton BZ, van Huysen TL. 2013. Evidence for progressive phosphorus limitation over long-term ecosystem development: examination of a biochemical paradigm. Plant Soil 367:135–47.

Jangid K, Whitman WB, Condron LM, Turner BL, Williams MA. 2013. Soil bacterial community succession during long-term ecosystem development. Mol Ecol 22:3415–24.

Jenny H. 1941. Factors of soil formation: a system of quantitative pedology. New York: McGraw-Hill. p 281.

Kendrick GW, Wyrwoll K-H, Szabo BJ. 1991. Pliocene-Pleistocene coastal events and history along the western margin of Australia. Quat Sci Rev 10:419–39.

Lajtha K, Schlesinger WH. 1988. The biogeochemistry of phosphorus cycling and phosphorus availability along a desert soil chronosequence. Ecology 69:24–39.

Laliberté E, Turner BL, Costes T, Pearse SJ, Wyrwoll K-H, Zemunik G, Lambers H. 2012. Experimental assessment of nutrient limitation along a 2-million-year dune chronosequence in the south-western Australia biodiversity hotspot. J Ecol 100:631–42.

Laliberté E, Grace JB, Huston MA, Lambers H, Teste FP, Turner BL, Wardle DA. 2013a. How does pedogenesis drive plant diversity? Trends Ecol Evol 28:331–40.

Laliberté E, Turner BL, Zemunik G, Wyrwoll K-H, Pearse SJ, Lambers H. 2013b. Nutrient limitation along the Jurien Bay dune chronosequence: response to Uren & Parsons (2013). J Ecol 101:1088–92.

Laliberté E, Zemunik G, Turner BL. 2014. Environmental filtering explains variation in plant diversity along resource gradients. Science 345:1602–5.

Lambeck K, Chappell J. 2001. Sea level change through the last glacial cycle. Science 292:679–86.

Lambers H, Shane MW, Cramer MD, Pearse SJ, Veneklaas EJ. 2006. Root structure and functioning for efficient acquisition of phosphorus: matching morphological and physiological traits. Ann Bot 98:693–713.

Lambers H, Raven JA, Shaver GR, Smith SE. 2008. Plant nutrient-acquisition strategies change with soil age. Trends Ecol Evol 23:95–103.

Lambers H, Cawthray GR, Giavalisco P, Kuo J, Laliberte E, Pearse SJ, Scheible W-R, Stitt M, Teste F, Turner BL. 2012. Proteaceae from severely phosphorus-impoverished soils extensively replace phospholipids with galactolipids and sulfolipids during leaf development to achieve a high photosynthetic phosphorus-use-efficiency. New Phytol 196:1098–108.

Lamont BB, Hopkins AJM, Hnatiuk RJ. 1984. The flora—composition, diversity and origins. In: Pate JS, Beard JS, Eds.

Kwongan: plant life of the sandplain. Nedlands: University of Western Australia Press. p 27–50.

Lamont BB, Maitre DCL, Cowling RM, Enright NJ. 1991. Canopy seed storage in woody plants. Bot Rev 57:277–317.

Lewis SE, Sloss CR, Murray-Wallace CV, Woodroffe CD, Smithers SG. 2013. Post-glacial sea-level changes around the Australian margin: a review. Quat Sci Rev 74:115–38.

Lichter J. 1998. Rates of weathering and chemical depletion in soils across a chronosequence of Lake Michigan sand dunes. Geoderma 85:255–82.

Lindsay WL, Norvell WA. 1978. Development of a DTPA soil test for zinc, iron, manganese, and copper. Soil Sci Soc Am J 42:421–8.

Lisiecki LE, Raymo ME. 2005. A Pliocene-Pleistocene stack of 57 globally distributed benthic $\delta^{18}O$ records. Paleoceanography 20:PA1003.

Loeppert RH, Suarez DL. 1996. Carbonate and gypsum. In: Sparks D et al., Eds. Methods in soil analysis, Part 3—Chemical methods. Madison: Soil Science Society of America. p 437–74.

Lowry DC. 1977. Perth Basin yellow sand. Search 8:54–6.

McArthur WM. 2004. Reference soils of south-western Australia. Perth: Department of Agriculture. p 285.

McArthur WM, Bettenay E. 1974. Development and distribution of soils of the Swan Coastal Plain, Western Australia. Canberra: CSIRO.

McArthur WM, Russell WGR. 1978. Soil morphological properties in relation to depth to groundwater table in a sandy landscape near Perth. Aust J Soil Res 16:347–9.

Mehlich A. 1984. Mehlich 3 soil test extractant: a modification of Mehlich 2 extractant. Commun Soil Sci Plant Anal 15:1409–16.

Melton JR, Mahtab SK, Swoboda AR. 1973. Diffusion of zinc in soils as a function of applied zinc, phosphorus, and soil pH. Soil Sci Soc Am J 37:379–81.

Menge DNL, Hedin LO. 2009. Nitrogen fixation in different biogeochemical niches along as 120 000-year chronosequence in New Zealand. Ecology 90:2190–201.

Miller KG, Kominz MA, Browning JV, Wright JD, Mountain GS, Katz ME, Sugarman PJ, Cramer BS, Christie-Blick N, Pekar SF. 2005. The Phanerozoic record of global sea-level change. Science 310:1293–8.

Murray-Wallace CV, Kimber RWL. 1989. Quaternary marine aminostratigraphy: Perth Basin, Western Australia. Aust J Earth Sci 36:553–68.

Myers N, Mittermeier RA, Mittermeier CG, da Fonseca GAB, Kent J. 2000. Biodiversity hotspots for conservation priorities. Nature 403:853–8.

Parfitt RL, Ross DJ, Coomes DA, Richardson SJ, Smale MC, Dahlgren RA. 2005. N and P in New Zealand soil chronosequences and relationships with foliar N and P. Biogeochemistry 75:305–28.

Peltzer DA, Wardle DA, Allison VJ, Baisden WT, Bardgett RD, Chadwick OA, Condron LM, Parfitt RL, Porder S, Richardson SJ, Turner BL, Vitousek PM, Walker J, Walker LR. 2010. Understanding ecosystem retrogression. Ecol Monogr 80:509–29.

Playford PE, Cockbain AE, Lowe GH. 1976. Geology of the Perth Basin, Western Australia. Bulletin 124 of the Geological Survey of Western Australia. Perth: Geological Survey of Western Australia.

Playford PE, Cockbain AE, Berry PF, Roberts AP, Haines PW, Brooke B. 2013. The geology of Shark Bay. East Perth: Geological Survey of Western Australia.

Prakongkep N, Gilkes RJ, Singh B, Wong S. 2012. Pyrite and other sulphur minerals in giant aquic spodosols, Western Australia. Geoderma 181–182:78–90.

Price DM, Brooke BP, Woodroffe CD. 2001. Thermoluminescence dating of aceolianites from Lord Howe Island and southwest Western Australia. Quat Sci Rev 20:841–6.

Salisbury EJ. 1925. Note on the edaphic succession in some dune soils with special reference to the time factor. J Ecol 13:322–8.

Selmants PC, Hart SC. 2008. Substrate age and tree islands influence carbon and nitrogen dynamics across a retrogressive semiarid chronosequence. Glob Biogeochem Cycles. doi:10.1029/2007GB003062.

Selmants PC, Hart SC. 2010. Phosphorus and soil development: does the Walker and Syers model apply to semiarid ecosystems? Ecology 91:474–84.

Semeniuk V, Searle DJ. 1986. Variability of Holocene sealevel history along the southwestern coast of Australia—evidence for the effect of significant local tectonism. Mar Geol 72:47–58.

Sniderman JMK, Jordan GJ, Cowling RM. 2013. Fossil evidence for a hyperdiverse sclerophyll flora under a non-Mediterranean-type climate. Proc Natl Acad Sci 110:3423–8.

Soil Survey Staff. 1999. Soil taxonomy: A basic system of soil classification for making and interpreting soil surveys. Lincoln: United States Department of Agriculture–Natural Resources Conservation Service.

Stevens PR, Walker TW. 1970. The chronosequence concept and soil formation. Q Rev Biol 45:333–50.

Stirling CH, Esat TM, Lambeck K, McCulloch MT. 1998. Timing and duration of the Last Interglacial: evidence for a restricted interval of widespread coral reef growth. Earth Planet Sci Lett 160:745–62.

Sulpice R, Ishihara H, Schlereth A, Cawthray GR, Encke B, Giavalisco P, Ivakov A, Arrivault S, Jost R, Krohn N, Kuo J, LalibertÉ E, Pearse SJ, Raven JA, Scheible W-R, Teste F, Veneklaas EJ, Stitt M, Lambers H. 2014. Low levels of ribosomal RNA partly account for the very high photosynthetic phosphorus-use efficiency of Proteaceae species. Plant Cell Environ 37:1276–98.

Syers JK, Adams JA, Walker TW. 1970. Accumulation of organic matter in a chronosequence of soils developed on wind-blown sand in New Zealand. J Soil Sci 21:146–53.

Tackett NW, Craft CB. 2010. Ecosystem development on a coastal barrier island dune chronosequence. J Coast Res 26:736–42.

Tapsell P, Newsome D, Bastian L. 2003. Origin of yellow sand from Tamala Limestone on the Swan Coastal Plain, Western Australia. Aust J Earth Sci 50:331–42.

Tejan-Kella MS, Chittleborough DJ, Fitzpatrick RW, Thompson CH, Prescott JR, Hutton JT. 1990. Thermoluminescence dating of coastal sand dunes at Cooloola and North Stradbroke Island, Australia. Aust J Soil Res 28:465–81.

Thompson CH. 1981. Podzol chronosequence on coastal dunes of eastern Australia. Nature 291:59–61.

Thompson CH. 1992. Genesis of podzols on coastal dunes in Southern Queensland: I. Field relationships and profile morphology. Aust J Soil Res 30:593–613.

Turner BL, Condron LM. 2013. Pedogenesis, nutrient dynamics, and ecosystem development: the legacy of T.W. Walker and J.K. Syers. Plant Soil 367:1–10.

Turner BL, Romero TE. 2009. Short-term changes in extractable inorganic nutrients during storage of tropical rain forest soils. Soil Sci Soc Am J 73:1972–9.

Turner BL, Condron LM, Richardson SJ, Peltzer DA, Allison VJ. 2007. Soil organic phosphorus transformations during pedogenesis. Ecosystems 10:1166–81.

Turner BL, Condron LM, Wells A, Andersen KM. 2012. Soil nutrient dynamics during podzol development under lowland temperate rain forest. Catena 97:50–62.

Vitousek PM. 2004. Nutrient cycling and limitation. Princeton: Princeton University Press.

Vitousek PM, Farrington H. 1997. Nutrient limitation and soil development: experimental test of a biogeochemical theory. Biogeochemistry 37:63–75.

Walker TW, Syers JK. 1976. The fate of phosphorus during pedogenesis. Geoderma 15:1–19.

Walker J, Thompson CH, Fergus IF, Tunstall BR. 1981. Plant succession and soil development in coastal sand dunes of subtropical eastern Australia. In: West DC, Shugart HH, Botkin DB, Eds. Forest succession: concepts and application. New York: Springer. p 107–31.

Walker LR, Wardle DA, Bardgett RD, Clarkson BD. 2010. The use of chronosequences in studies of ecological succession and soil development. J Ecol 98:725–36.

Wardle DA, Walker LR, Bardgett RD. 2004. Ecosystem properties and forest decline in contrasting long-term chronosequences. Science 305:509–13.

Wardle DA, Bardgett RD, Walker LR, Peltzer DA, Lagerström A. 2008. The response of plant diversity to ecosystem retrogression: evidence from contrasting long-term chronosequences. Oikos 117:93–103.

Wells A, Goff J. 2007. Coastal dunes in Westland, New Zealand, provide a record of paleoseismic activity on the Alpine fault. Geology 35:731–4.

White PJ. 2012. Long-distance transport in the xylem and phloem. In: Marschner P, Ed. Marschner's mineral nutrition of higher plants. London: Academic Press. p 49–70.

Williamson WM, Wardle DA, Yeates GW. 2005. Changes in soil microbial and nematode communities during ecosystem decline across a long-term chronosequence. Soil Biol Biochem 37:1289–301.

Woods PJ, Searle DJ. 1983. Radiocarbon dating and Holocene history of the Becher/Rockingham Beach ridge Plain, West Coast, Western Australia. Search 14:44–6.

Wyrwoll KH, King PD. 1984. A criticism of the proposed regional extent of Late Cenozoic arid zone advances into south-western Australia. Catena 11:273–88.

Wyrwoll K-H, Turner BL, Findlater P. 2014. On the origins, geomorphology and soils on the sandplains of south-western Australia. In: Lambers H, Ed. Plant life on the sandplains in Southwest Australia, a global biodiversity hotspot. Crawley: University of Western Australia Publishing. p 3–23.